Fall 2019

Design, synthesis, characterization and anti-cancer effects evaluation of interchain cysteine linked antibody drug conjugates

Ke Li

Department: Chemistry

DESIGN, SYNTHESIS, CHARACTERIZATION AND ANTI-CANCER EFFECTS EVALUATION OF INTERCHAIN CYSTEINE LINKED ANTIBODY DRUG CONJUGATES

by

KE LI

A DISSERTATION

Presented to the Graduate Faculty of the

MISSOURI UNIVERSITY OF SCIENCE AND TECHNOLOGY

In Partial Fulfillment of the Requirements for the Degree

DOCTOR OF PHILOSOPHY

in

CHEMISTRY

2019

Approved by:

Yinfa Ma, Advisor
Honglan Shi, Co-Advisor
Paul Nam
Jeffrey G. Winiarz
Zhongping (John) Lin

PUBLICATION DISSERTATION OPTION

This dissertation consists of the following three articles, formatted in the style used by the Missouri University of Science and Technology:

Paper I, found on pages 22-41, has been published in *Analytical Chemistry 91.13 (2019): 8558-8563.*: Ke Li, Yinfa Ma, Zhongping (John) Lin and Honglan Shi. Characterization of Positional Isomers of Interchain Cysteine Linked Antibody−Drug Conjugates by High-Resolution Mass Spectrometry.

Paper II, found on pages 42-63, has been submitted to *Journal of Analytical and Bioanalytical Chemistry (Accepted)*: Ke Li, Zhiling Zhang, Zhongping (John) Lin, Yinfa Ma and Honglan Shi. Accurate Determination of Drug to Antibody Ratio of Interchain Cysteine Linked Antibody Drug Conjugates by LC−HRMS.

Paper III, found on pages 64-78 is intended for submission to *Molecular Pharmaceuticals*: Ke Li, Zhiling Zhang, Zhongping (John) Lin, Yinfa Ma and Honglan Shi. Design, Synthesis and Toxicity Study of Cetuximab-Staurosporine on Non-Small Cell Lung Cancer Cells.

ABSTRACT

Antibody drug conjugates (ADCs) are emerging therapeutic products specially designed for the treatment of cancers. Potent cytotoxic agents are linked to antibodies via linkers. Antibody drug conjugates, which take advantage of both antibodies and cytotoxic agents, showed high selectivity towards cancer cells. Cytotoxic agents are delivered to the cancer cells selectively and kill them from inside while leaving low or non-toxicity towards normal cells. Antibody drug conjugates are actually heterogeneous mixtures. The major heterogeneities mainly lie in the drug to antibody ratio (DAR) and drug linking positions, both of which potentially affect the therapeutic index of ADCs. In this research, we focused on the interchain cysteine linked ADCs, which are the most popular class. We first developed methods and characterized the drug linking position heterogeneity. Positional isomers of interchain cysteine linked ADCs were separated and their relative abundance was determined. In addition, novel LC/HRMS methods were developed for the accurate determination of the DAR with cleavable and non-cleavable linkers. Meanwhile, we also designed and synthesized new ADCs, namely Cetuximab-Staurosporine for EGFR over expressed Non-Small Cell Lung Cancer. The anticancer effects were evaluated on A549 human lung cancer cells.

ACKNOWLEDGMENTS

I would like to express my gratitude to my advisor Dr. Yinfa Ma and my co-advisor Dr. Honglan Shi. I have learned not only fundamental knowledge, but also experimental skills, logical thinking abilities, problem solving abilities, communication skills, and leadership abilities during my Ph.D. studies. My advisors also encouraged me to attend conferences to enrich my research perspective and provide me opportunities to collaborate with colleagues working in the same area. Everything I have learned from them will benefit my whole life.

I would like to express my gratitude to Dr. Mu Chen and Dr. Zhiling Zhang from Frontage Laboratories. This work would never have been completed without their help. This work was supported by funds from Frontage Laboratories, Inc. I am very thankful for the financial support and assistance.

I would like to express my gratitude to my doctoral committee members Dr. Paul Nam, Dr. Jeffrey G. Winiarz and Dr. Zhongping (John) Lin for the various ways in which they have assisted me.

I would like to thank Dr. Qingbo Yang, Dr. Haiting Zhang, Mrs. Kun Liu, Dr. Wenyan Liu, Xiaolong He and my other group members for their help. I would also like to thank Dr. Li Tan, Dr. Shengsheng Xu, Dr. Euhu Lu, and Dr. Tina Li from Frontage Laboratories for their support and help in my research. Finally, I want to express my deep gratitude to my friends and family for their support and encouragement.

TABLE OF CONTENTS

Page

LIST OF ILLUSTRATIONS

SECTION Page

LIST OF TABLES

1. INTRODUCTION

1.1. CANCER AND CHEMOTHERAPY

Cancer is a major public health problem worldwide and is the second leading cause of death in the United States.[1] In the past year, 1,762,450 people were diagnosed with cancer and 606,880 patients died in United States.[1] The overall survival rate was quite low, with some cancer as low as less than 20%. Surgery that removed tumor was desired the treatment method for cancer. However, many of the cancers were diagnosed in later stages where the use of surgery was limited. Instead, chemotherapeutic agents such as DNA damaging agents, tubulin inhibitors and antifloate agents were applied for treatment.[2-4] Chemotherapeutic agents usually lack specificity to tumor cells with their selectivity relying on the relatively higher uptake rate of rapidly growing cancer cells than that of normal cells.[3] In addition to the disadvantage that many patients developed acquired resistance to the chemotherapeutic agents, one significant drawback of those agents were their toxicities to normal tissues, especially normal tissues characterized with enhanced proliferation rate.[3-4] Medicinal chemists and oncologists have long sought ways to increase the delivery of cytotoxic chemicals to cancer cells for increased efficacy, while minimizing the exposure of normal healthy tissue.[5-6]

1.2. ANTIBODY DRUG CONJUGATES

Antibody drug conjugates are emerging target therapeutic products specially designed for cancer treatment. The concept of antibody drug conjugates can be dated back to 1980s when there was a need to improve the selectivity of chemotherapy drugs.[7]

Antibody drug conjugates are sophisticated drug delivery systems that deliver anticancer agents to the cancer cells selectively.[8] An ADC consists of three components: monoclonal antibody (mAb), linker and cytotoxic agent (Figure 1.1).[9] The cytotoxic agent is linked to the surface of the antibody by a linker, which forms covalent bonds at both ends with functional groups on the antibody and cytotoxic agents. Monoclonal antibodies that govern selectivity act as the drug carrier to deliver the cytotoxic agent to the tumor cells where the cytotoxic agents take action, which trigger cell apoptosis.[9-10]

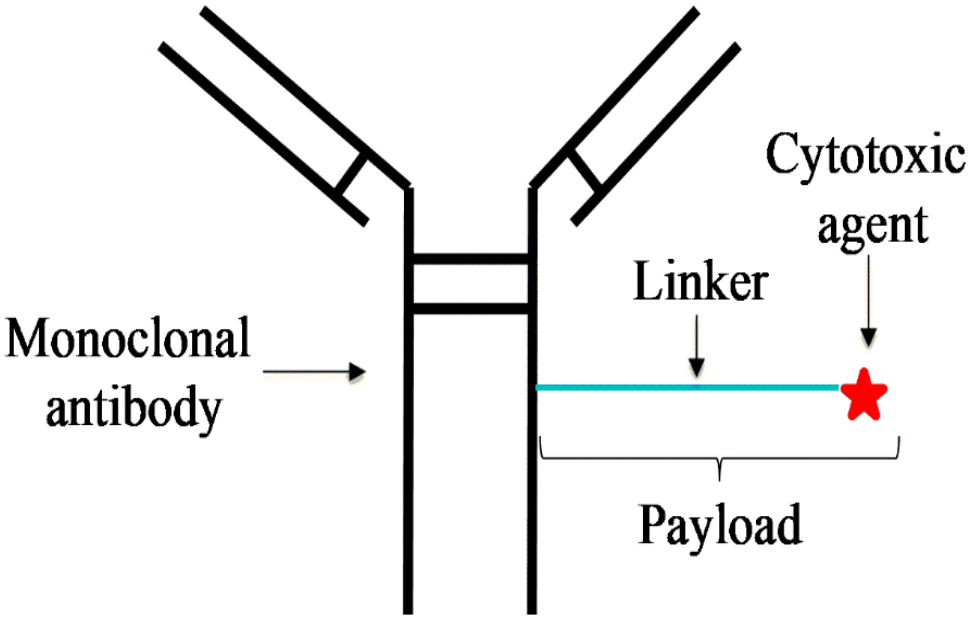

Figure 1.1. Structure of antibody drug conjugates.

Antibody drug conjugates take advantages of both antibody and cytotoxic agents, greatly enhancing the selectivity and lowering systematic toxicity toward health cells.[11] Antibody drug conjugates were promising target therapeutics for the treatment of cancers. Currently, four ADCs have been approved by FDA for the treatment of various cancers.

1.2.1. Antibody. Antibodies, also known as immunoglobulins, are big biological proteins mainly produced in plasma B cells and are important components of the immune system. There are five types of immunoglobulins in human beings, namely IgM, Ig D, Ig G, Ig A and Ig E. These immunoglobulins are close related glycoprotein with the exception of the heavy chain structure and effectors function. Among these immunoglobulins, IgG accounts for about 80% of the total immunoglobulin and is the most abundant immunoglobulin in blood. IgG can be further divided to four subclasses in order of decreasing abundance: IgG1, IgG2, IgG3 and IgG4. As a major component of IgG and is responsive to membrane proteins, IgG1 has attracted a lot of attention for developing antibody drug conjugates. In ADCs, the antibodies were almost exclusively IgG1.

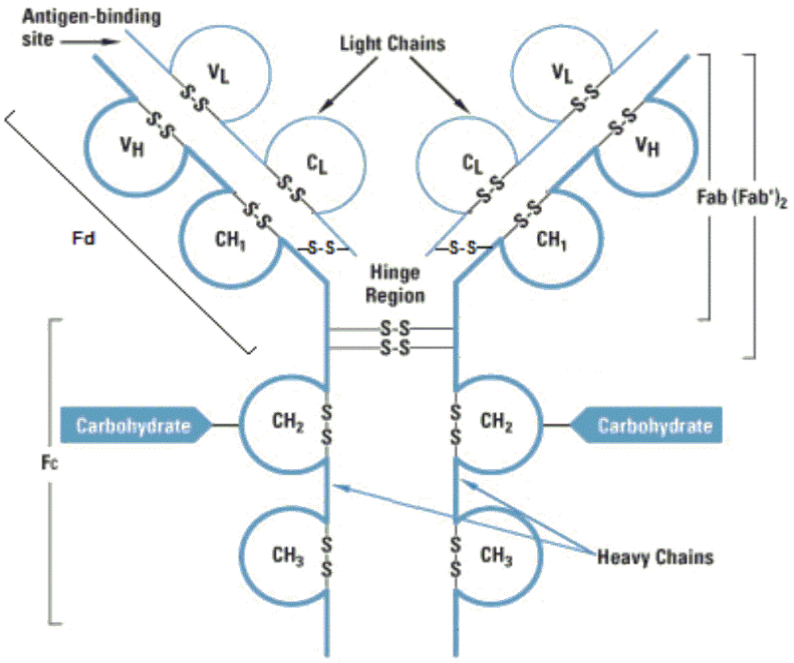

Figure 1.2. Structure of human IgG1.
(https://www.thermofisher.com)

As shown in Figure 1.2, IgG1 is a Y shaped glycoprotein molecule with a MW of about 150 K Da. It has two light chains and two heavy chains with length of roughly 210 and 450 amino acids, respectively. In IgG1, there are two glycans attached on the asparagine residues located at the CH2 region of the Fc domain,[12] it has folded structure under native condition where the hydrophobic fragments are buried inside while the hydrophilic fragments are exposed outside. This makes IgG1 a good aqueous soluble molecule. IgG1 also has 16 pairs of interchain disulfide bonds, which are buried inside of the folded structure and are not solvent accessible under native condition. It also contains four pairs of interchain disulfide bonds, two of which are between light chain and heavy chain while the other two are located in the hinge region between the heavy chains.

Table 1.1. Amino acids sequence of constant region of human IgG1.

Name	Sequence
Kappa Light Chain Constant	RTVAAPSVFI FPPSDEQLKS GTASVVCLLN NFYPREAKVQ WKVDNALQSG NSQESVTEQD SKDSTYSLSS TLTLSKADYE KHKVYACEVT HQGLSSPVTK SFNRGEC
Lambda Light Chain Constant	GQPKANPTVT LFPPSSEELQ ANKATLVCLI SDFYPGAVTV AWKADGSPVK AGVETTKPSK QSNNKYAASS YLSLTPEQWK SHRSYSCQVT HEGSTVEKTV APTECS
Heavy Chain Constant	ASTKGPSVFP LAPSSKSTSG GTAALGCLVK DYFPEPVTVS WNSGALTSGV HTFPAVLQSS GLYSLSSVVT VPSSSLGTQT YICNVNHKPS NTKVDKKVEP KSCDKTHTCP PCPAPELLGG PSVFLFPPKP KDTLMISRTP EVTCVVVDVS HEDPEVKFNW YVDGVEVHNA KTKPREEQYN STYRVVSVLT VLHQDWLNGK EYKCKVSNKA LPAPIEKTIS KAKGQPREPQ VYTLPPSRDE LTKNQVSLTC LVKGFYPSDI AVEWESNGQP ENNYKTTPPV LDSDGSFFLY SKLTVDKSRW QQGNVFSCSV MHEALHNHYT QKSLSLSPGK

Structurally, IgG1 consists of one variable region and three constant regions. The variable region is located at the top of two arms. It consists of VL and CL, which interact with each other and form three complementarity-determining regions that determine the specificity of the antibody. The unique structure at the end of the variable region was the antigen binding site where the antibody binds to antigen and forms a complex. IgG1 also contains several constant regions, namely CL and CH1-3. Compared to the variable region, the constant regions were universal to all the IgG1, and their sequence and structure were kept constant regardless of the variation in the variable region. IgG1 has a single type of heavy chain and two types of light chains, which are Kappa or Lambda. Their amino acid sequences of the constant region were shown in Table 1.1.

1.2.2. Linker. Linker is a vital component that impacts the effectiveness of ADCs.[13] Structurally, linker acts as a bridge that joins the antibody and anticancer agents together. It has active functional groups on both ends and is capable of reacting with functional groups of both antibody and anticancer agents. Linkers need to possess two key attributes: stability during circulation and drug release after internalization.[6, 14] Linkers should be sufficiently stable enough to maintain the cytotoxic agents attached on the antibody to provide extended circulation time, and to enhance drug localization to cancer cells. Meanwhile, linkers should prevent the premature release of cytotoxic agents, which usually lack selectivity, are harmful to healthy cells, and lower the therapeutic efficacy.[6] After internalization, the ADCs should efficiently release the active drugs to change ADCs from pro-drugs to active drugs.[15] The form of active drug varies depending on the linker types. Linkers can be characterized as cleavable linkers (Figure 1.3), which are susceptible to acidic pH or lysosomal enzyme and can be cleaved in lysosome to release the cytotoxic

agents,[16-19] or as non-cleavable linkers (Figure 1.3), which rely on the complete digestion of the antibody backbone to release the payload linked with the amino acid that it is attached to.[20-21]

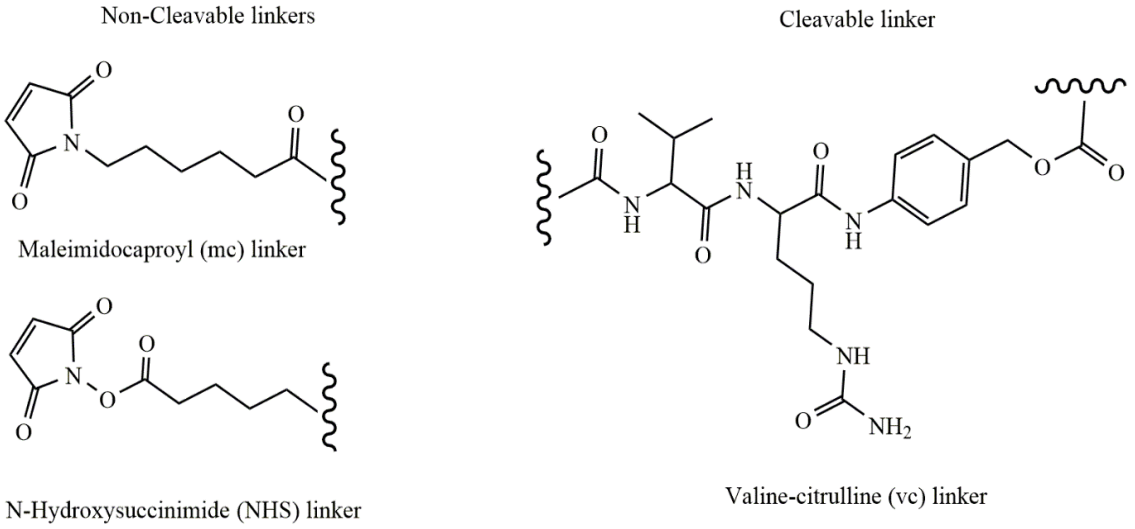

Figure 1.3. Non-cleavable and cleavable linkers.

In addition, the hydrophobicity of the payload, which is partly due to the linker, is also an important factor that affect the efficacy of ADCs.[22] The payload of ADCs is usually hydrophobic, and linking of payload to the antibody adds additional hydrophobicity to the antibody.[23] This may induce aggregation, which has been linked to increased immunogenicity and hepatotoxicity.[23-24] Meanwhile, the hydrophobic nature of the payload makes it a good target for multidrug resistant transporters.[23] It has been reported that a hydrophilic linker enhanced the effectiveness of DM1, a hydrophobic anticancer agent.[25]

1.2.3. Cytotoxic Agents. Unlike traditional chemotherapy drugs, the cytotoxic agents employed in ADCs must be highly toxic to kill tumor cells at very low

concentrations considering the number of antigens expressed on the tumor cell surface and the fact that limited anticancer agents can be linked on antibody without severely compromising the physical and pharmacokinetics of ADCs.[14, 26] The cytotoxic agents used in ADCs have toxicities that are usually at nM or pM level.[26-27]

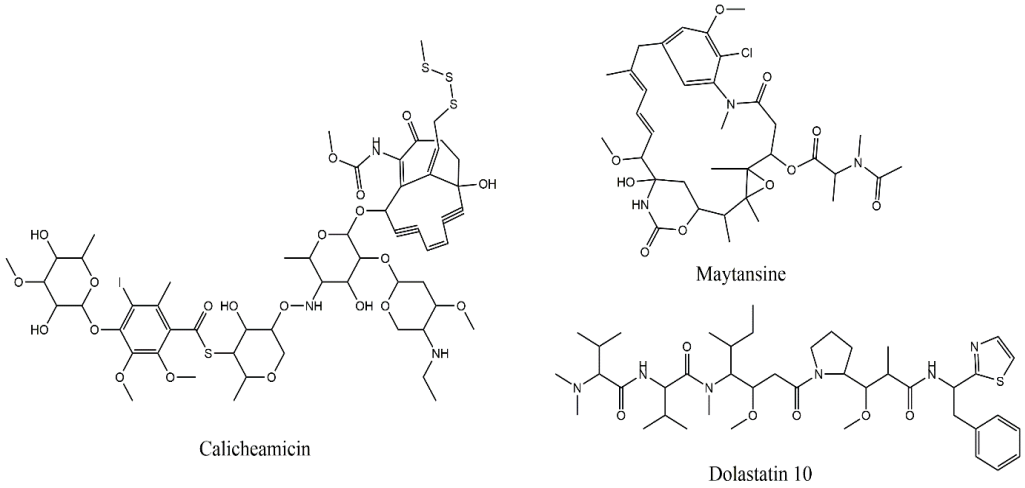

Figure 1.4. Cytotoxic agents of ADCs.

Current cytotoxic agents employed in ADCs are usually derivatives of calicheamicin (Figure 1.4), which kill cells by interacting with DNA and introducing DNA double strand breaks to trigger cell apoptosis.[14, 28] They also may be derivatives of dolastatin 10 and maytansine (Figure 1.4), a family of antimitotic microtubule disrupting agents that inhibit the cell mitosis and trigger cell apoptosis.[27, 29-31]

1.3. MECHANISM OF ACTION OF ADCS

The mechanism of action of ADCs involves in several steps, which are depict in Figure 1.5.[23] After administration, ADCs circulate in the vein and diffuse to the cancer

cells with expressed antigens on their surfaces. The ADCs recognize the antigen, or more specifically the epitope on the antigen, and bind to it tightly, forming an ADC/antigen complex. The complex then undergoes a process called internalization via receptor-mediated endocytosis.

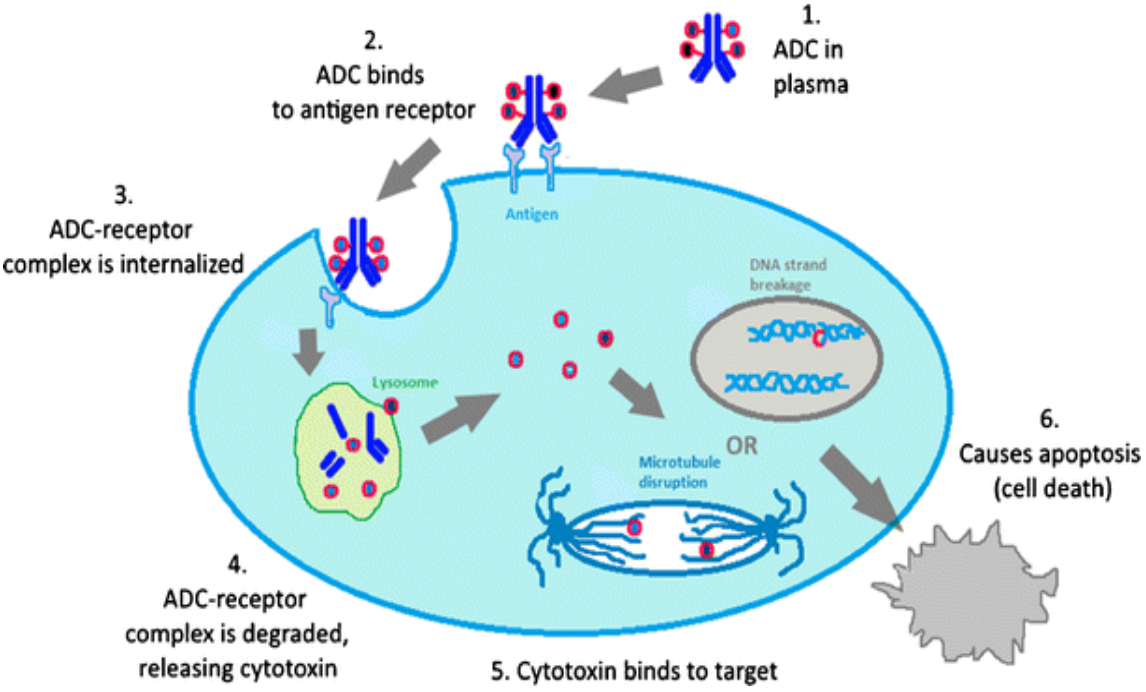

Figure 1.5. Action mechanism of antibody drug conjugates.

The internalized ADCs are subsequently transferred to late endosome and form lysosome, which has an acidic environment and contains multiple enzymes. The following protease digestion transferred the ADCs from the pro-drug form to active drug form by digesting the linker or peptide back bone, depending on the linker types. The active drugs that are released into the cytoplasm bind to specific organelles or structures, usually DNA and microtubules, to trigger cell apoptosis and thus kill the cancer cells from the inside.

ADCs are sophisticated drug delivery systems specially designed to deliver the cytotoxic drugs to cancer cells and kill them, while leaving normal cells mostly unaffected.

1.4. ADC CLASSIFICATION

Antibodies are large protein molecules that maintain folded structure under native conditions. That structure plays a critical role in the functioning of ADCs. Therefore, antibodies cannot be denatured during drug conjugation, so limited functional groups can be used for payload conjugation, considering the available functional groups on the surface of the antibody. ADCs can be divided into three classes based on the drug linking methods. Figure 1.6 displays the three types of ADCs, namely lysine linked ADCs, interchain cysteine linked ADCs, and engineered cysteine linked ADCs.[32]

In lysine linked ADCs, payload is linked on the lysine, more specifically, the amine group located at the end of the side chain.[23, 33] Human IgG1 mAb contains about 16 lysines on the surface of the antibody, which are solvent accessible and therefore may be linked with payloads. In addition to lysine, cysteine linking was another popular method. Human IgG1 contains four pairs of interchain disulfide bonds, which are not very important for the stability of the antibody. In interchain cysteine linked ADCs, the payloads are linked on the interchain cysteine, taking advantage of the click chemistry between maleimide and thiol. The reduction of a disulfide bond generates two free thiols, which may be linked with two payloads.[34] Even though the four pairs of interchain disulfide bonds are not very important for the stability of the antibody, disruption of those disulfide bonds potentially lowers the stability of the antibody.[35] Instead of employing native cysteine, the engineered antibody contains two extra cysteines which are inserted in the sequence of the antibody

during manufacturing.[36] The payloads are linked on the inserted cysteines, and the native disulfide bonds are not disturbed.[34] Among all these ADCs, interchain cysteine linked ADCs are the most popular one due to their relatively narrow drug to antibody ratio (DAR) distribution and good therapeutic index.

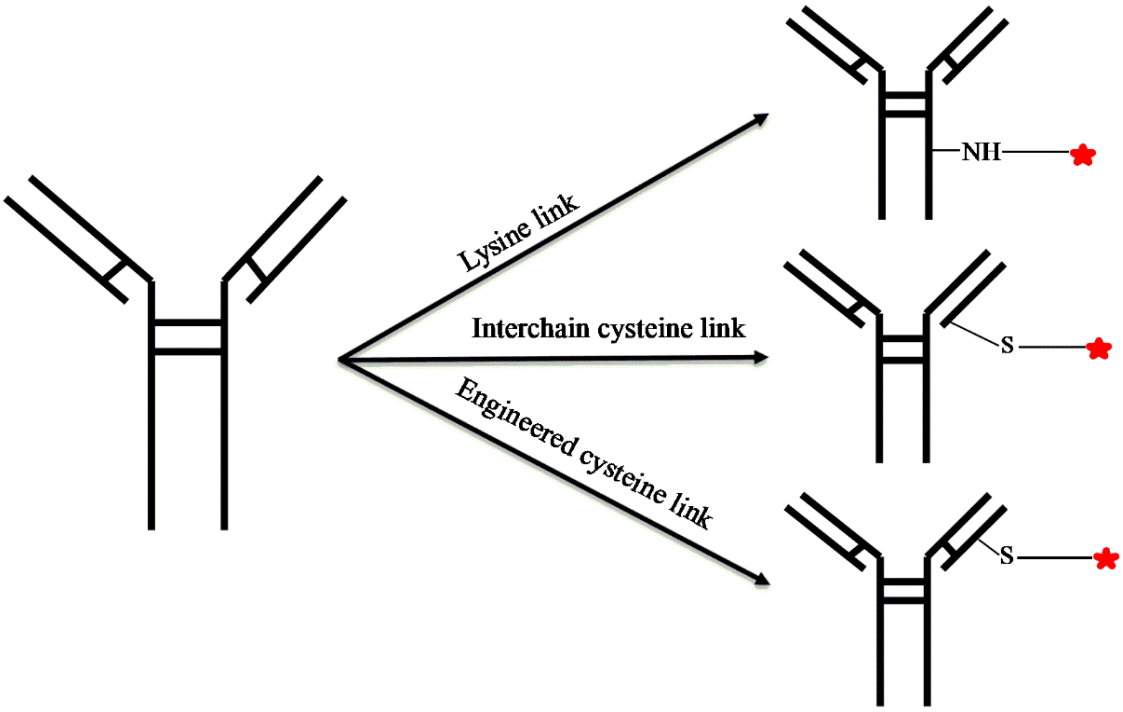

Figure 1.6. Antibody drug conjugation classification.

1.5. ADC MANUFACTURE

Manufacture of the interchain cysteine linked ADCs requires several steps as shown in Figure 1.7. In human IgG1, all interchain cysteines are paired and there have no free thiols for drug conjugation. Therefore, the interchain disulfide bonds need to be reduced to active thiol before conjugation. Limited amounts of DTT or TCEP are added to the antibody solution to partially reduce the interchain disulfide bonds to active free thiols.[37]

Afterwards, the excessive DTT or TCEP is removed. Payloads that composed of linkers and drugs are added to the reduced antibodies for conjugation. The maleimide moiety of the payload reacts readily with the thiol and forms stable a covalent bond. As a consequence, the payload was firmly linked on the antibody.

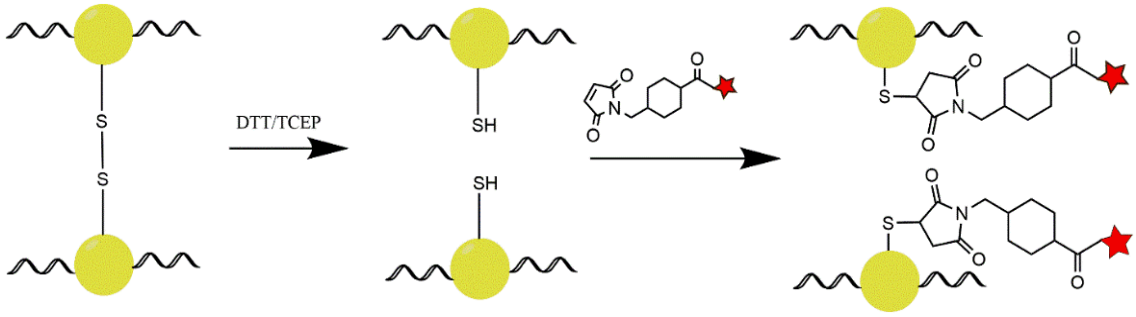

Figure 1.7. Manufacture of interchain cysteine linked ADCs.

Reduction of one disulfide bond generates two free thiols and therefore can be linked with two payloads. Depending on the random reduction of the interchain disulfide bonds, the antibody might be linked with 0, 2, 4, 6 or 8 payloads.[37]

1.6. ADCS HETEROGENEITY

The heterogeneity of the interchain cysteine linked ADCs mainly lies on drug linking numbers and drug linking positions.[34, 38] In the manufacturing process, the interchain disulfide bonds of the antibody are randomly reduced, and therefore the antibody might be linked with 0, 2, 4, 6, or 8 drugs (Figure 1.8) depending on the reduction of the interchain disulfide bonds.

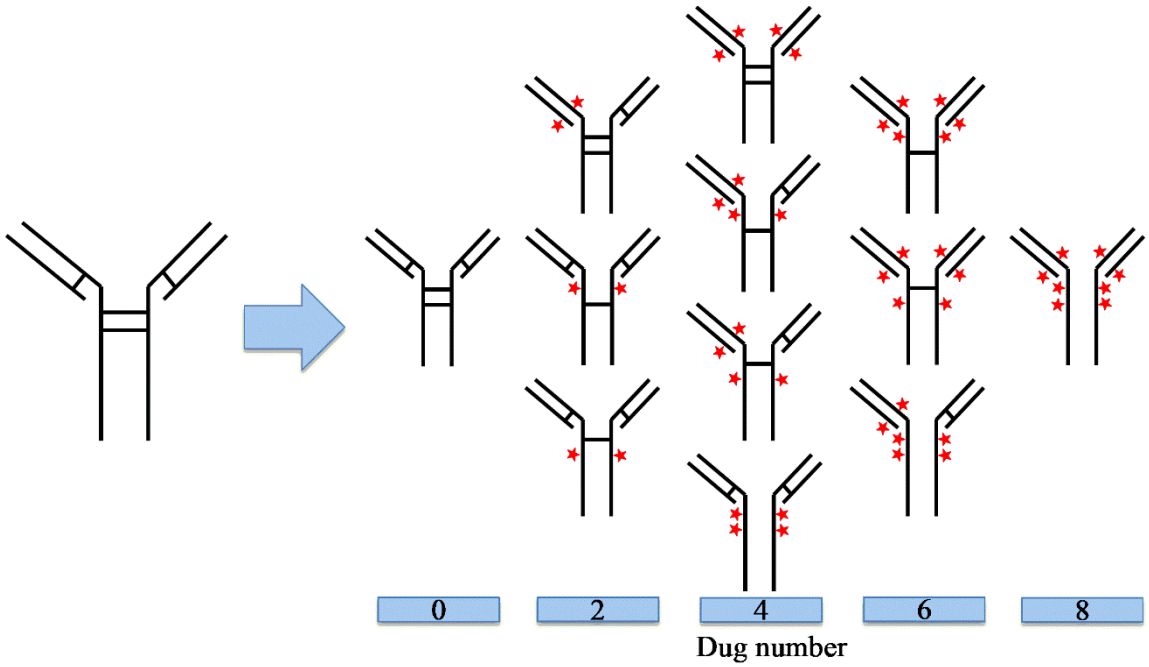

Figure 1.8. Heterogeneity of interchain cysteine linked antibody drug conjugates.

It is obvious that the number of cytotoxic drugs linked on antibody is proportional to the number of drugs delivered to the cancer cells, and therefore the drug linking number is a vital parameter directly affecting the therapeutic efficacy.[39] Theoretically, the more drug linking on the antibody, the better therapeutic effect would be expected. However, the drug linking number also affects the therapeutic effects by its impact on the hydrophobicity of the ADCs.[22] The payloads employed in ADCs are usually hydrophobic, and therefore linking of payloads to the antibody increased the hydrophobicity of the antibody. This tends to cause the ADCs to aggregate, while the aggregation not only decreases the efficacy of the ADCs but also increases the risk of hepatotoxicity.[23-24] In a clinical trial of an interchain cysteine linked ADCs, ADCs with an average drug number of 4 showed similar therapeutic efficacy to ADCs linked with 8 drugs, which revealed that the faster blood clearance rate

of ADCs linked with more drugs.[40] The drug linking number is a critical factor that affect the efficacy of the ADCs in multiple ways.

In addition to the drug linking number, the drug linking position is another major heterogenity. Even though the same number of drugs are linked on the antibodies, the drugs linking positions might be different (Figure 1.8). Drug linking positions might potentially affects the stability of the ADCs and therefore influence the therapeutic efficacy.[41] In interchain cysteine linked ADCs, the conjugation is via maleimide-thiol reaction. However, the reaction is reversible even though the reverse reaction rate is very low. Human blood contains plenty of albumin (contains one active thiol) and other free active thiols. The active thiols compete with the antibody for drugs.[42] In a clinical trial, it was found the drug was transferred to albumin, which indicated the deconjugation of the payload from antibody.[42] Drug deconjugation not only reduced the potency of the ADCs, but also enhanced the off-target toxicity since the deconjugated drug doesn't have selectivity.[43] Baldwin et al. investigated the conjugation stability of the maleimide and thiol reaction and found that the reactivity of the thiol is related to the stability of the conjugation.[44] Later, Shen and coworkers found that the deconjugation of the drug from the antibody was largely affected by the solvent accessibility.[45] The more water accessible the linking position is, the more easy it is to cause drug deconjugation.[45] Difference of drug linking positions actually potentially affects the therapeutic efficacy.

1.7. ADC CHARACTERIZATIONS

The characterization of interchain cysteine linked ADCs is challenging. The interchain disulfide bonds are disrupted during manufacture, which makes the ADCs

susceptible to acid and organic solvents. Antibody drug conjugates are easily denatured by any harsh conditions, which makes the characterization more difficult. Hydrophobic interaction chromatography (HIC) – UV/Vis that operates under non-denaturing condition is a good choice for characterization.[46-47] Different DAR species can be separated and the drug number can be determined by extinction coefficient of antibody and payload. However, HIC is not compatible with mass spectrometer and therefore unable to confirm the mass of each species. In recent years, high resolution mass spectrometry (HRMS) has become popular technique for the characterization of interchain cysteine linked ADCs.[48-50] The ADCs may be characterized by HRMS in three ways, as shown in Figure 1.9, namely top down, middle down and bottom up.[51]

In top down characterization, ADCs are directly analyzed by HRMS under non-denaturing conditions in which the ADCs still maintain an intact structure.[52] The raw mass spectra of the ADCs contains several species with multiple charge states. It is difficult to directly interpret the mass spectra. Instead, the raw mass spectra is processed with software to obtain the deconvoluted mass spectra, in which same species with different charge states are deconvoluted to one peak displaying the molecular weight. HRMS is effective to differentiate different DAR species, but it fails to provide any drug linking position information. Size exclusion chromatography (SEC) using volatile salts are compatible with HRMS and can be used for separation. However, the mass differences between different species are limited, usually 1-3 KDa. The differences are too small to achieve full separation considering the large molecular weights of intact ADCs which are about 150 K Da.[53]

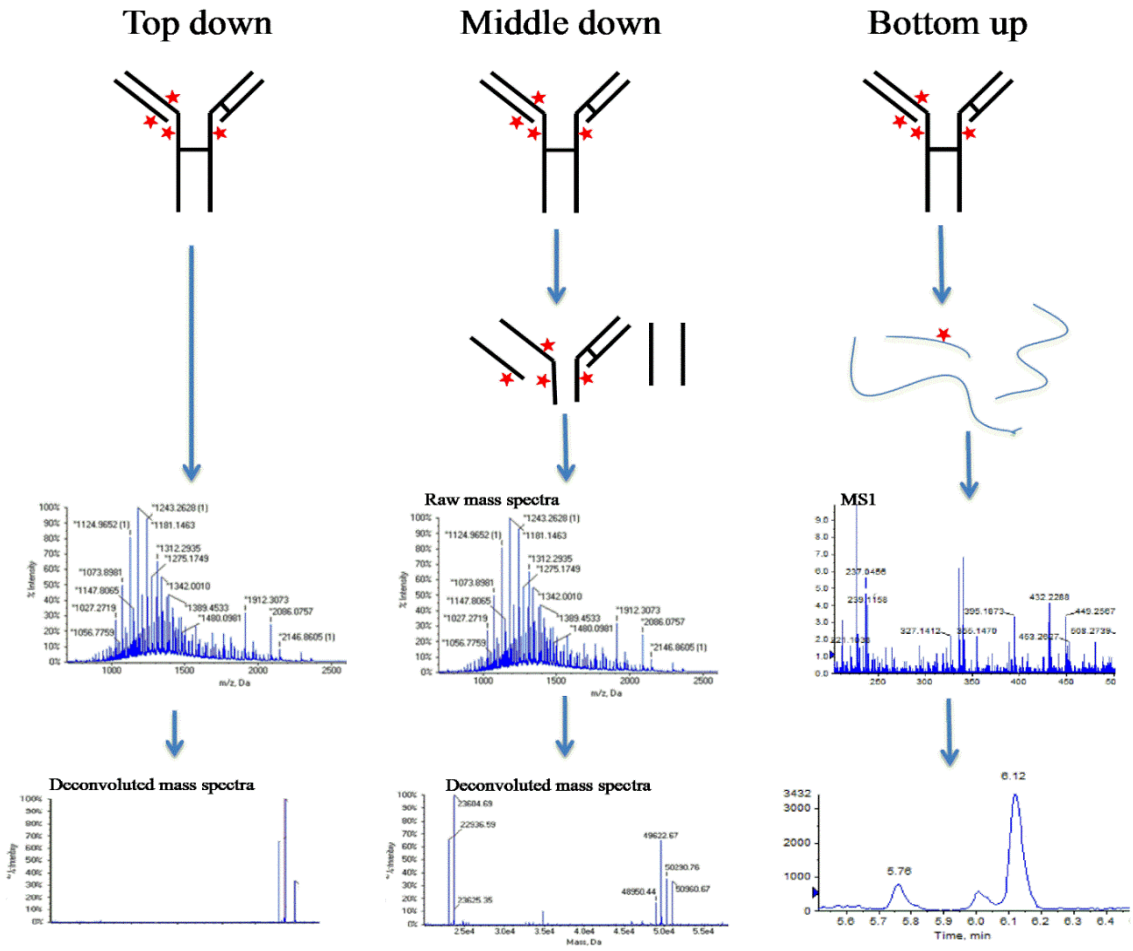

Figure 1.9. Top down, middle down and bottom up characterization of ADCs.

Middle down is another popular characterization method. It is similar to the top down method but has some differences in the sample preparation. In middle down characterization, the ADCs are digested to relatively shorter fragments that contain more information regarding the drug linking positions and drug distribution.[49] Unlike top down method, the middle down method is compatible with denaturing condition, therefore RPLC may be used for separation of different species. Even though it is hard to fully separate all the fragments, the middle method is still able to provide plenty of information regarding the drug distribution information.

In bottom up method, the ADCs are digested by enzymes, usually trypsin, chymotrypsin or Glu-C, into short peptides that have mass ranging from hundreds to thousands Da. The short peptides contain more detailed information regarding drug linking positions, modifications on the backbone of the ADCs.[54] The combination of RPLC and HRMS makes the bottom up strategy a powerful method to provide more detailed information regarding minor modifications on the ADCs. Meanwhile, when standard is employed, the bottom up analysis of ADCs is extended from qualitative analysis to quantitative analysis, which greatly supports the characterization of ADCs.[55]

1.8. DRUG TO ANTIBODY RATIO DETERMINATION

Drug to antibody ratio is a vital factor of the ADCs and therefore needs to be accurately determined. HIC-UV/Vis or UV/Vis methods are considered gold standard methods for the measurement of DAR.[46, 52] The DAR can be calculated based on the abundance of each DAR species or the extinction coefficient of antibody and payload.[40] However, these methods require large amounts of samples and high ADC concentration because of the low sensitivity of UV/Vis detectors. Meanwhile, those methods are easily affected by matrix and therefore usually not applicable to clinical samples. Recently, high resolution mass spectrometry (HRMS) has attracted lot of attention for DAR determination. HRMS analysis of the ADCs at intact or subunit level provides a feasible way to determine the DAR.[48, 56] However, the DAR is a rough estimation rather than a accurate determination.

In HRMS analysis, the DAR is calculated based on the abundance of each species while under the assumption that different DAR species have the same mass response.[48, 56]

However, high DAR species have relatively lower ionization efficiency and therefore results in lower mass response. Chen et al. compared the DAR calculated by HIC-UV/Vis and HRMS as shown in Table 1.2.[52] The abundances of high DAR species in HRMS analysis were much lower than those in HIC-UV/Vis analysis.[52] Accurate determination of DAR by HRMS is still challenging due to the ionization efficiency variations of different DAR species.

Table 1.2. DAR profile of Native HRMS and HIC of interchain cysteine linked ADCs.

native nano-ESI MS			HIC		
drug load	peak area (%)	weighted peak area (%)	drug load	peak area (%)	weighted peak area (%)
0	11.5	0	0	6.2	0
2	37.4	74.8	2	31.0	62.0
4	46.5	186	4	48.9	195.6
6	3.8	22.8	6	11.7	70.2
8	0.8	6.4	8	2.1	16.8
DAR		2.9	DAR		3.4

1.9. NON-SMALL CELL LUNG CANCER

Lung cancers are the leading causes of cancer related death in the United States. It is estimated that there are 234,000 new cases and 154, 000 deaths per year.[57] Despite the new therapies that has been developed in recent years, the 5-year survival rate is very low only 18%.[58] Among lung cancers, non-small cell lung cancers (NSCLC) was a major type that accounts for 85% of the lung cancers.[59] Several therapies were developed for the treatment of NSCLC. Surgery that removed the tumor was the most desired therapy. However, more than half of the NSCLC patients were diagnosed at advanced stage or metastasis state where the benefit of surgery was limited. Instead, chemotherapy became

the dominant treatment therapy.[59-60] However, chemotherapy was frequently associated with drug resistance where cancer cells developed acquired resistance to the chemotherapy drugs.[61-62] Meanwhile, severe side effects were observed in almost all patients receiving chemotherapy due to the non-selectivity of the chemotherapy drugs.[63] While killing the cancer cells, many healthy cells were also affected. Actually, chemotherapies only showed modest survival benefits during the late stage lung cancer treatment.[64-65] Developing target therapies is in high demand for the treatment of NSCLC to overcome the disadvantages of the chemotherapy.

EGFR is a transmembrane protein expressed on the surface of cells.[66] It has been associated with tumor proliferation, metastasis and suppression of apoptosis.[67] It has a low level of expression in normal tissue,[68] but, there has been abnormally high expression of EGFR in some NSCLC patients.[69] Approximately 25% of the lung cancer patients were detected with over expressed EGFR in tumor cells (IHC score $\geq$300).[69] The large difference in EGFR expression between normal cells and tumor cells made it a good target for specially targeting lung cancer cells that have over-expressed EGFR.

1.10. CETUXIMAB

Cetuximab is a mouse/human chimerical IgG1 antibody developed in the late 1990s. Similar to human IgG1, the constant region of the Cetuximab is the same as human IgG1. However, the variable region of the Cetuximab is specially developed, which can specially recognize and bind to the extracellular domain of EGFR (Figure 1.10 A).[70]

Cetuximab binds the EGFR at the EGF binding site and therefore competes with EGF.[70] However, Cetuximab showed limited therapeutic benefit for NSCLC treatment in

clinical trials.[71] Despite its poor therapeutic effects, Cetuximab has high affinity to both wild type and EGFRVIII mutated EGFR, and the Kd is only 0.38 nM.[72] It seems promising to employ Cetuximab to specially targeting the EGFR overexpressed NSCLC.

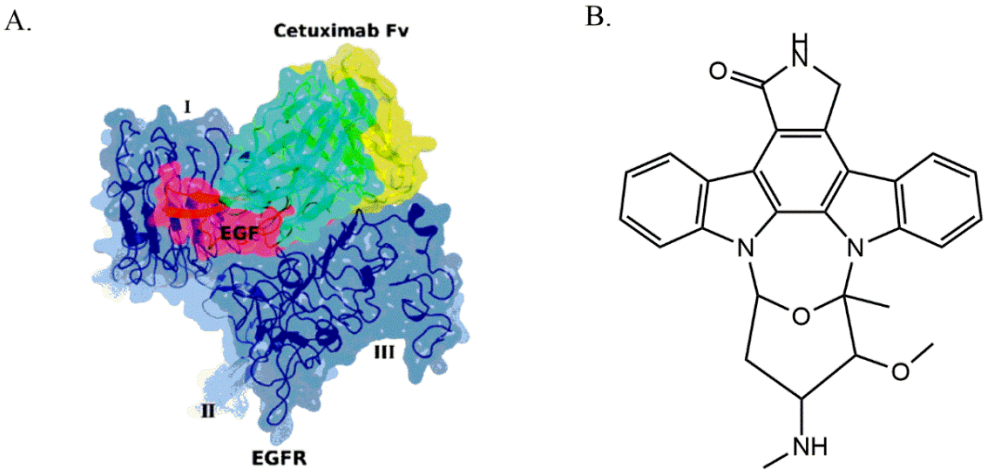

Figure 1.10. Structure of Cetuximab, EGFR, EGF and Staurosporine.
(A) Variable region of Cetuximab interact with EGFR. (B) Structure of Staurosporine.

1.11. STAUROSPORINE

Since discovered in 1982, Staurosporine (STS, Figure 1.10B) has attracted a lot of attention for the treatment of cancers.[73-74] However, its poor selectivity has limited its application in pharmaceutical application.[75] STS has very high affinity toward cyclin dependent kinase 2 (CDK2), an important protein involved in cell division cycle, and the IC50 is only 3.2 nM.[76-77] STS binds to the CDK2 at the ATP binding site and mimics the hydrogen bonds made by the adenine moiety of ATP. After binding to CDK2, the moieties of STS form several hydrogen bonds with Glu 81, Leu 83, Asp 86 and Gln131, forming a stable complex.[76] Meanwhile, the complex forms a very hydrophobic

environment that has poor solvent accessibility, which inhibits the binding of ATP to CDK2. Thus, the function of CDK2 is inhibited and it fails to phosphorylate downstream proteins. Therefore cells are arrested at the end of G1 phase or G2 phase.[78] Incubation of A549 lung cancer cells with 4 nM STS for 2 days induced about 50% of the cell growth inhibition.[79] Cells were found to be arrested at G1 and G2/M phases, and cell apoptosis was observed.[79-80] It was found that STS induced two Casp 3 dependent and one Casp 3 independent pathways of apoptosis.[81-82] STS is an interesting compound that kills cancer cells by inducing cell division inhibition. However, additional methods to increase the selectivity toward cancer cells are required.

1.12. CETUXIMAB-STAUROSPORINE

Cetuximab-Staurosporine (Figure 1.11) that possesses the advantages of both Cetuximab and Staurosporine seems to be a very promising anticancer drugs for the treatment of EGFR over expressed NSCLC.

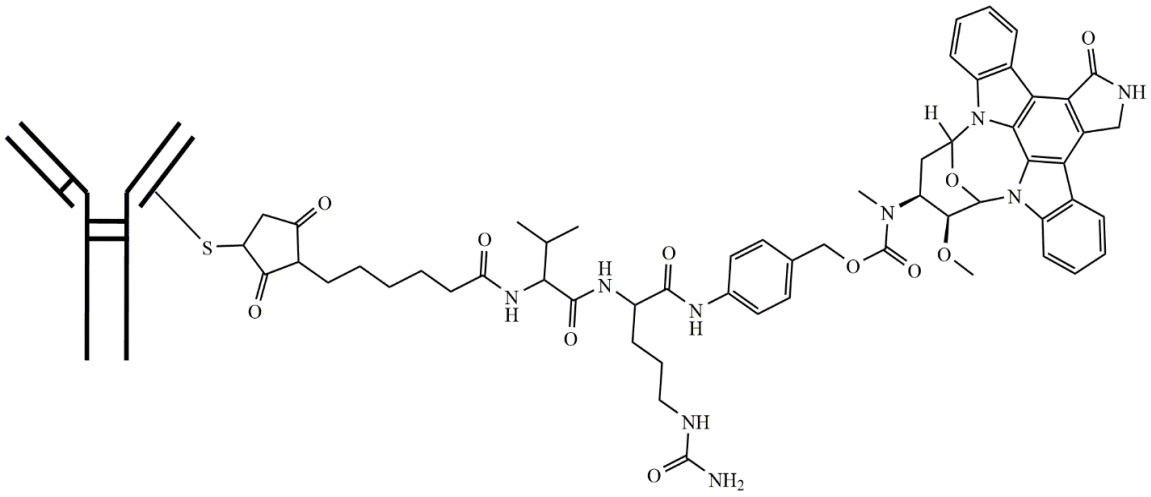

Figure 1.11. Schematic show of Cetuximab-Staurosporine.

The antibody portion is expected to selectively recognize and bind to the EGFR over expressed cancer cell, and further deliver the toxic STS into the cancer cells. The STS would bind to the CDK2 and inhibit its function. The cells would be expected to be arrested at G1 and G2 phase and further induce apoptosis. Cetuximab-Staurosporine would be interesting ADCs and it would be worthful to investigate its effectiveness the on treatment of EGFR overexpressed NSCLC.

1.13. RESEARCH OBJECTIVE

This work aims to develop analytical method for characterization and drug to antibody determination of interchain cysteine linked ADCs, as well as design, synthesis and anticancer effectiveness investigation of ADCs. The whole work including three parts:

(1) Characterization of positional isomers of interchain cysteine linked ADCs. Subunit analysis and bottom up analysis were combined to analyze the drug distribution, separate positional isomers and identify drug linking positions.

(2) Accurate determination of drug to antibody ratio of interchain cysteine linked ADCs with cleavable or non-cleavable linkers.

(3) Design, synthesis and anticancer effectiveness investigation of ADCs. New ADCs, Cetuximab-Staurosporine, were synthesized and characterized. The anticancer effectiveness was investigated on A549 human lung cancer cells.

PAPER

I. CHARACTERIZATION OF POSITIONAL ISOMERS OF INTERCHAIN CYSTEINE LINKED ANTIBODY DRUG CONJUGATES BY HIGH RESOLUTION MASS SPECTROMETRY

Ke Li[1], Zhongping (John) Lin[2], Honglan Shi[1], Yinfa Ma[1, 3*]

[1]Department of Chemistry and Center for Biomedical Research, University of Missouri, Rolla, MO, 65409

[2]Department of Bioanalysis, Frontage Laboratories, Inc., Exton, PA, 19341

[3]Department of Chemistry, California State University, Sacramento, CA 95819

ABSTRACT

Interchain cysteine linked antibody drug conjugates (ADCs) are emerging therapeutic products that antagonize with cancers. The toxic payloads are selectively linked to the interchain cysteines but generate heterogeneous mixtures of positional isomers. These positional isomers might contribute differently to the therapeutic efficacy due to the variation of conjugation stability and thus need to be well characterized. However, the characterization of the positional isomers of interchain cysteine linked ADCs is very challenging mainly due to the high similarity between those isomers. In this research, we developed a novel mass spectrometry method for characterization of positional isomers of interchain cysteine linked ADCs. The subunit analysis and the bottom-up analysis provided abundant information about the drug numbers and drug linking positions on each chain. Since the method can provide accurate data on drug linking numbers and positions on each

chain, it will be very useful for researchers in cancer drug development and cancer treatment.

Abstract Figure:

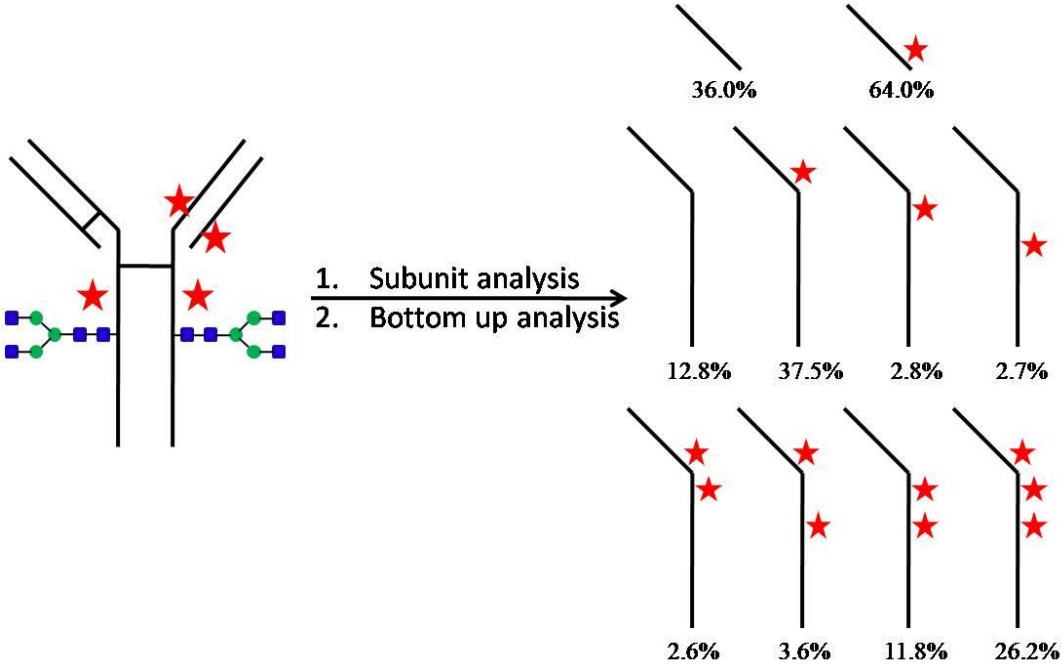

1. INTRODUCTION

Antibody drug conjugates (ADCs) are novel therapeutic products that combine monoclonal antibodies (mAb) and cytotoxic small molecules for treatment of cancers[1]. The toxic drug molecules were linked to lysine or cysteine on the mAb via a cleavable or non-cleavable linker[2]. The conjugates can target specific cancer cells and greatly enhance the selectivity of the drug molecules (cytotoxic payload) while maintaining other cells being affected as less as possible [1,3]. The success of brentuximab vedotin and

trastuzumab emtansine greatly inspired pharmaceutical companies to develop new ADC products[4]. Currently, there are more than 65 ADCs that antagonize with cancers are under clinical trials and more are under pre-clinical developments[5, 6]. Among these ADCs, about two-third of them are interchain cysteine linked ADCs based on the disclosed information[7]. The interchain cysteine linked ADCs are manufactured by partial reduction of the 4-pair interchain disulfide bonds which are not very important for the stability of the antibody, followed by alkylation of reduced sulfhydryl function group with maleimide linker that connected with cytotoxic drug at the other end[8, 9]. Depending on the reduction of the interchain disulfide bonds, the antibody may be linked with 0, 2, 4, 6 and 8 drugs and usually with average of 4 drugs/antibody considering the hydrophobicity increments of the drug loading. Conjugation of drug molecules to the antibody increased the structural complexity and thus requires comprehensive characterization of the ADCs.

Current methods for characterization of interchain cysteine-linked ADCs mainly focus on the drug to antibody ratio (DAR) and drug distribution,[10-12] size and charge variants,[13, 14] and biophysical properties.[15, 16] Little attention is paid on the positional isomers. Even though the thiol-maleimide conjugation is stable under in vitro environment, deconjugation often happens in vivo due to the thiol exchange with reactive thiols of the albumin, free cysteine and glutathione[17, 18]. Aaron D. Baldwin† and Kristi L. Kiick investigated the stability of thiol-maleimide in the presence of glutathione and found that the thiol-maleimide conjugation stability is strongly related with the reactivity of thiol group[19]. The reactivity of the thiols on antibody is mainly affected by the amino acid sequence and the functional groups near the thiol group, which indicates that the linking position potentially affects the stability of the antibody-drug conjugation. The study

by Shen BQ, Xu K, Liu L, Raab H, Bhakta S, Kenrick M, Parsons-Reponte KL, Tien J, Yu SF, Mai E et al demonstrated that the deconjugation of maleimide from thiol was closely related to the linking positions[18].The drug was much easier to be deconjugated at solvent accessible linking positions comparing to those of relatively not solvent accessible positions.[18] Drug deconjugation during circulation reduced the potency of ADCs which partly depend on the extent of drug linkage on mAb.[20, 21] Meanwhile, systemic exposure of the deconjugated drug might adversely affect the safety of the ADCs due to the non-selectivity of the deconjugated drug.[20, 22]

Characterization of positional isomers of interchain cysteine linked ADCs is very challenging mainly due to the structural similarities. Direct analysis of ADCs at intact levels using multi-dimensional liquid chromatography UV mass spectrometry (LC-UV/MS) has been developed for separation of different DAR species[23, 24]. However, the method was not sufficient to separate all the positional isomer of same DAR species. Even though chromatography separation of reduced ADCs can separate light chain (LC) and heavy chain (HC) with different drug-linked species, it is not able to separate all of the HC + 1 drug and HC + 2 drugs positional isomers[9, 25]. It was reported that treatment of ADCs with IdeS to remove the Fc portion can improve the separation of positional isomers[25, 26], but the HC + 1 drug and HC + 2 drugs positional isomers still cannot be fully separated. In this research, we developed a novel mass spectrometry method, as shown in Figure 1, for characterization of positional isomers of interchain cysteine linked ADCs, which provides important information regarding drug number and linking position on each chain by combining ADCs subunit analysis with the bottom-up analysis. The LC and HC positional isomers can be fully separated and their amounts can be determined.

This novel analytical method will be very useful for cancer drug discovery, development and cancer treatment.

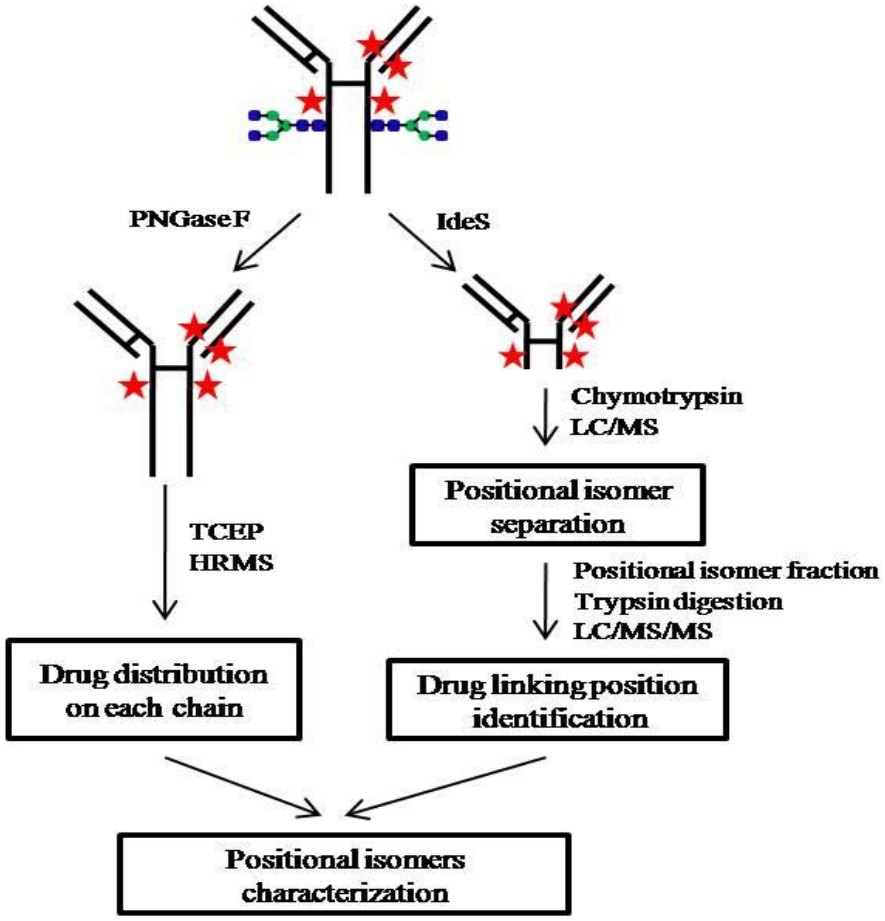

Figure 1. The schematic showing of characterization of positional isomers of interchain cysteine linked ADCs.

2. EXPERIMENTAL SECTIONS

2.1. RAGENTS AND MATERIALS

The deionized water was generated using a Millipore water purification system (Burlington, MA). Sodium hydroxide (NaOH) (1.0 M), isopropanol, and LC/MS grade

formic acid, acetonitrile (ACN) were obtained from Fisher Scientific (Fair Lawn, NJ); tris (2-carboxyethyl) phosphine (TCEP) was purchased from Thermo Fisher Scientific (Rockford, IL), and 1.0 M tris buffers (pH 7.4 and 8.0) were obtained from Invitrogen (Austin, TX). IdeS, PNGase F (10,000 unit/mL), trypsin and chymotrypsin were purchased from Promega Corporation (Madison, WI). Urea, Iodoacetamide, CaCl2 and ADCs (mAb-SMCC-LC-Dansyl) were obtained from sigma Aldrich (St. Louis, MO).

2.2. ADC DEGLYCOSYLATION

ADCs were deglycosylated under non-denatured condition. Briefly, 4 µL of ADCs solution containing 20 µg of ADCs and 2 µL of the PNGase F solution were added to 14 µL of 50 mM tris buffer (pH 7.4). The mixture was incubated overnight at 37 ^{o}C.

2.3. IDES DIGESTION

Briefly, 4 µL of ADCs solution containing 20 µg of ADCs and 2 µL of IdeS enzyme solution containing 20 unit of IdeS were added to 34 µL of 50 mM tris buffer (pH 7.4). The mixture was incubated at 37 ^{o}C for 1.0 hour.

2.4. ADC SUBUNIT ANALYSIS

Prior to mass spectroscopy analysis, the deglycosylated or IdeS digested ADCs were treated with 5 mM TCEP for 30 min for reduction. Afterwards, 1 µg of the reduced ADCs was injected onto column for separation (Waters XBridge protein BEH C4, 3.5 µm, 2.1 x 50 mm, 300 Å). A Shimadzu LC-30 system employing deionized water containing 0.1% formic acid as mobile phase A and ACN containing 0.1% formic acid as mobile phase B was used for separating the analytes. The flow rate was set at 0.3 mL/min. 3.0 min of

isocratic elution with 5% mobile phase B was used for online desalting. The analytes were then eluted from column using 70% mobile phase B. The LC system was coupled with AB Sciex 6600 (QTOF) high resolution mass spectrometer (HRMS) operating in positive mode with ion spray voltage of 5000 V and temperature of 500 °C. Acquisitions were performed on mass rang of m/z 800-4000 with 1.0 s accumulation time and bin of 40.

2.5. DRUG LINKING PEPTIDES SEPARATION

The IdeS treated ADCs were denatured by 6.0 M urea under 37 °C for 1.0 hour in the presence of 5.0 mM TCEP for reduction. Then, 25.0 mM of iodoacetamide was added for alkylation over 30 min in the dark. Prior to chymotrypsin digestion, the sample was diluted with digestion buffer (50 mM tris with 10% ACN and 10 mM CaCl2, pH 8.0) to make urea concentration be less than 1.0 M. Chymotrypsin was then added as 1/50 (enzyme/substrate) ratio to the mixture and the digestion was performed overnight at 25 °C. Formic acid was added up to 0.5% to quench the digestion.

The digest was loaded onto a Waters ACQUITY BEH C18 column (1.7 µm, 2.1 x 50 mm, 130 Å) that was heated at 50 °C. The peptides were separated by a Shimadzu LC30 system. Mobile phase A was water containing 0.1% formic acid and mobile phase B was ACN containing 0.1% formic acid. The flow rate was controlled at 0.3mL/min. 2.0 min isocratic elution with 5% mobile phase B was applied for desalting and then the peptides were eluted from column by increasing mobile phase B to 50% within 10.0 min. An AB Sciex 6600 QTOF HRMS equipped with ESI ionization source was used for data acquisition.

2.6. DRUG LINKING POSITIONS IDENTIFICATION

To analyze the drug linking positions, the fractions of each HC positional isomer resulting from chymotrypsin digestion were collected. 1.0 M NaOH solution was added to neutralize the formic acid in the solution and the solution was further diluted with 100 mM tris buffer (pH 8.0) until ACN content was less than 20%. Then, 1.0 µg of trypsin was added to the solution and the peptides were digested with rapid enzyme digestion system at 37 °C for 30 min. After digestion, formic acid was added (up to 0.5%) to quench the digestion. Isopropanol was also added (up to 20%) to prevent drug containing peptides from precipitation. Then, 50 µL of digest was injected onto a Waters column (Acquity BEH C18, 1.7 µm, 2.1 x 50 mm, 130 Å) for separation. A 2.0 min isocratic elution with 5% mobile phase B was used for desalting, and then the peptides were eluted from the column by increasing mobile phase B to 90% within 10.0 min. MS analysis was performed on an AB Sciex 6600 QTOF HRMS with ESI ionization source, the detection was performed under positive ion mode in m/z from 150 to 2500 with heating temperature at 500°C and IS voltage at 5000 V.

3. RESULTS AND DISCUSSION

3.1. DRUG DISTRIBUTION ASSESSMENT

PNGase F specifically cleaved the glycans and recovered the glycosylated asparagine back to aspartic acid thus eliminated the adverse effect of the glycans on the mass analysis. The further TCEP treatment reduced the interchain disulfide bonds to free thiols in the free LC and HC species. As a consequence, the LC may be linked with 0 or 1

drug, while the HC may be linked with 0-3 drugs. Each drug linkage contributed approximate 668 Da mass increase. Figure 2A showed the raw mass spectra of the deglycoslyated ADCs. The raw mass spectra were processed with BioPharmaView software and generated the deconvolution mass spectra as shown in Figure 2B.

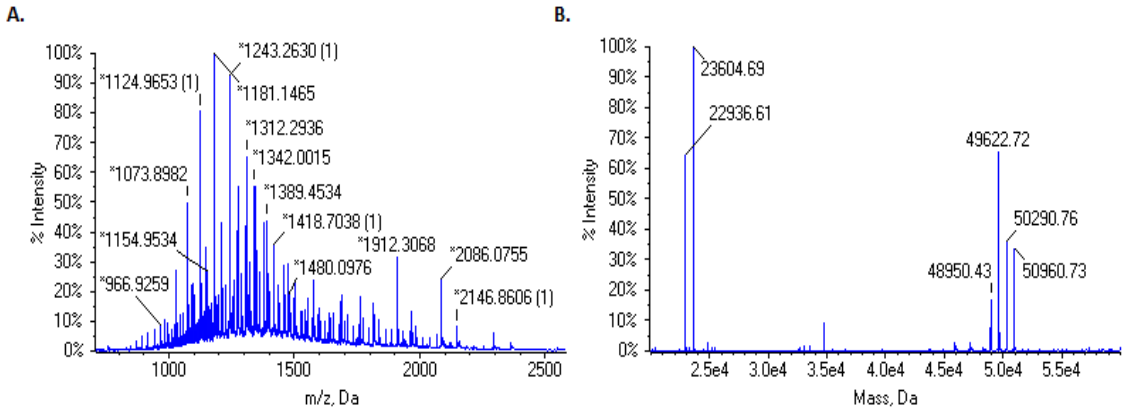

Figure 2. Subunit analysis of ADCs. Raw mass spectra (A) and deconvoluted mass spectra (B) of deglycosylated ADCs.

The LC was detected with MW of 22936.33 Da and LC + 1 drug was detected at 23603.68 Da with a mass increase of 667.35 Da. Likewise, HC species were detected with MW of 48949.02 Da, the HC drug linked species were detected at 49616.93 Da, 50285.73 Da and 50953.01 Da with mass increase of 667.73 Da, 1336.71 Da, and 2003.99 Da, which matched well with the mass shift of 1, 2, and 3 drug molecules. The abundance of each species was calculated by their peak areas. 64.0% of the LC were linked with 1 drug and the remaining 36.0% were linked with no drug. 12.8%, 43.0%, 18%, and 26.3% of the HC were linked with 0, 1, 2, and 3 drugs, respectively.

The HRMS analysis of the ADCs at subunit level provided a feasible way to directly determine the drug distribution on each chain. In this analysis, it was assumed that all the LC or HC species with different drug linkage have same mass response. While, it is worth to note that the drug linkage and number of drug on the chains may have some effects on their mass response and thus might potentially compromise the accuracy of the method.

3.2. IDES DIGESTION

IdeS is an enzyme modified from Streptocoocus Pyogenes that is frequently used for the characterization and ADCs[26, 27]. It specifically cleaves human IgG1 antibody at the two consecutive glycine positions and produces Fab fragments with all the drug linking positions and Fc with glycans. The F(ab)2 fragments were further reduced by TCEP to generate free LC and Fd species. As a consequence, the LC species were linked with 0-1 drug and Fd fragments were linked with 0-3 drugs.

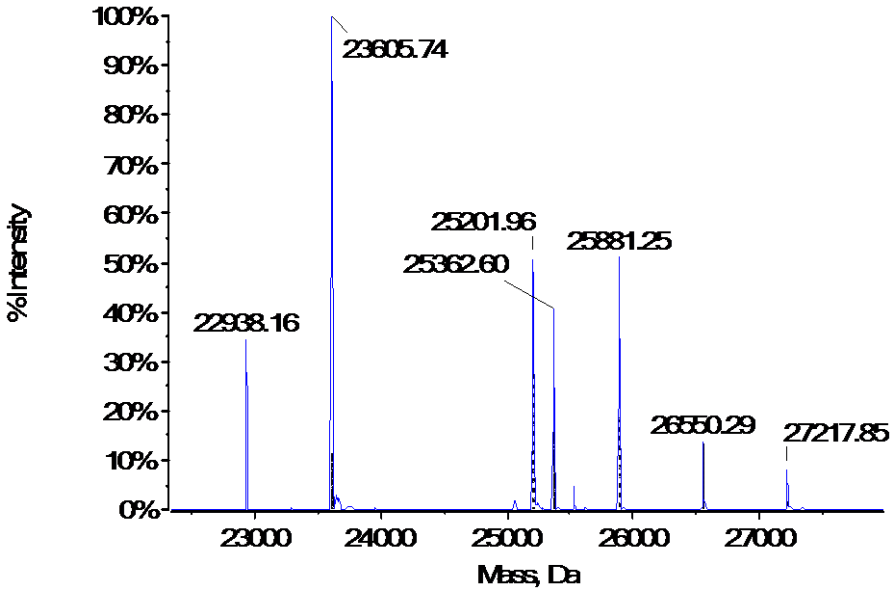

Figure 3. Deconvoluted mass spectra of IdeS treated ADCs.

Figure 3 presented the deconvoluted mass spectra of IdeS treated ADCs. Fd was detected with MW of 25201.96 Da, Fd + 1 drug, Fd + 2 drugs, and Fd + 3 drugs species were detected at 25881.25 Da, 26550.29 Da and 27217.85 Da, which matched well with the mass shift of approximate 668 Da/drug. The detection of all the Fd species indicated that the drug linkage on the interchain cysteines didn't interfere with the function of IdeS. Meanwhile, all of the HC species disappeared after IdeS treatment, which indicated the complete digestion of the heavy chains regardless of the drug linkage.

3.3. SEPARATION OF DRUG LINKING PEPTIDES

In the subunit analysis, the distribution of different species and their abundances were easy to recognize. However, the HC +1 drug and HC +2 drugs species are actually mixture of 3 positional isomers and the individual isomers were not able to be monitored. The separations of those isomers were very difficult due to the long peptide and high similarity between the positional isomers, especially the hinge region position isomers which were only 2 amino acids apart. Instead of direct separation of those isomers, chymotrypsin that specifically cleave protein at the Y/W/F position was employed to digest the heavy chain to peptides for LC-MS analysis. The chymotrypsin digestion of HC results in peptide of HC_203-245 which preserved all the 3 drug linking positions that located at Cys_224, 230, and 233. Initially, direct chymotrypsin digestion of ADCs was performed using a typical protocol involving in 6.0 M urea denaturation, 5.0 mM TCEP reduction, 25.0 mM iodoacetamide alkylation and chymotrypsin digestion (enzyme/substrate =1/50). However, the results showed very low intensity of 1 and 2 drug linked positional isomers. The downstream peptide next to the drug linking peptide was also detected with very low

intensity comparing with the antibody digestion results. Therefore, the drug linkage on the interchain cysteines may potentially decreased the chymotrypsin cleavage efficiency at Phe_245 position. In this study, the ADCs were treated with IdeS first to completely digest the heavy chains at Gly_240 position, which eliminated the low digestion efficiency at Phe_245 position issue.

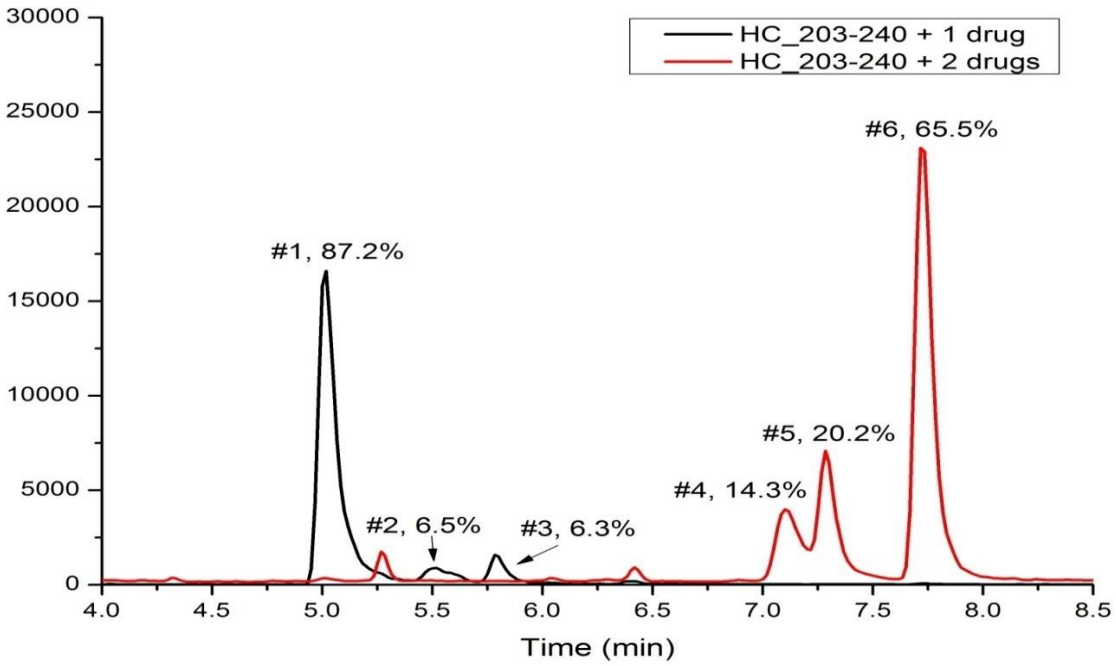

Figure 4. Chromatography separation of heavy chain positional isomers.

After IdeS digestion, the Fab fraction was further digested with chymotrypsin. The chymotrypsin digestion of the Fab fraction resulted in HC_203-240 peptide that was linked with 0-3 drugs. The relative short peptide enlarged the positional isomer differences and thus made it easier to separate them by using gradient elution, which was demonstrated in Figure 4. Peaks #1-3 that corresponding to HC_203-240 +1 drug positional isomers were detected at 5.01 min, 5.55 min, and 5.79 min, respectively. Their relative abundances were

calculated to be 87.2%, 6.5% and 6.3% based on their peak areas. Meanwhile, peaks #4-6 that corresponding to the three HC_203-240 +2 drugs positional isomers were detected at 7.11 min, 7.29 min, and 7.73 min with relative abundances of 14.3%, 20.2% and 65.5%.

3.4. DRUG LINKING POSITIONS IDENTIFICATION

To determine the peaks #1-6 drug linking positions, the analytes were fragmented and the fragment masses were compared with theoretical masses. However, no significant fragments with drug linkage were observed and thus unable to determine the drug linking positions. This may probably due to the long peptide sequence and resistance of fragmentation near drug linking positions. To solve this problem, the positional isomers, instead of direct fragmentation, were collected and further digested with trypsin. Trypsin digestion resulted in SCDK and THTCPPCPAPELLG peptides which preserved the drug linking positions. The relatively short peptides were used for drug linking position analysis.

In the analysis of the positional isomers digests, peak #1 analyte digest was detected with SCDK + 1 drug and bear THTCPPCPAPELLG peptides, which indicated the drug linkage on Cys_224. Peak #6 analyte digest was detected with THTCPPCPAPELLG + 2 drugs which confirmed the drug linkage on both Cys_230 and Cys_233. Peak #2 and Peak #4 analyte digests were both detected with THTCPPCPAPELLG +1 drug with retention time at 6.01 min (showed in Figure 5A). So, they have the same drug linkage position on the THTCPPCPAPELLG peptide. Similarly, the peak #3 and peak #5 analyte digests were also detected with THTCPPCPAPELLG +1 drug, but with different retention time at 6.12 min (Figure 5B). The peak # 3 and peak #5 seemed having the same drug linking positions on the THTCPPCPAPELLG peptide.

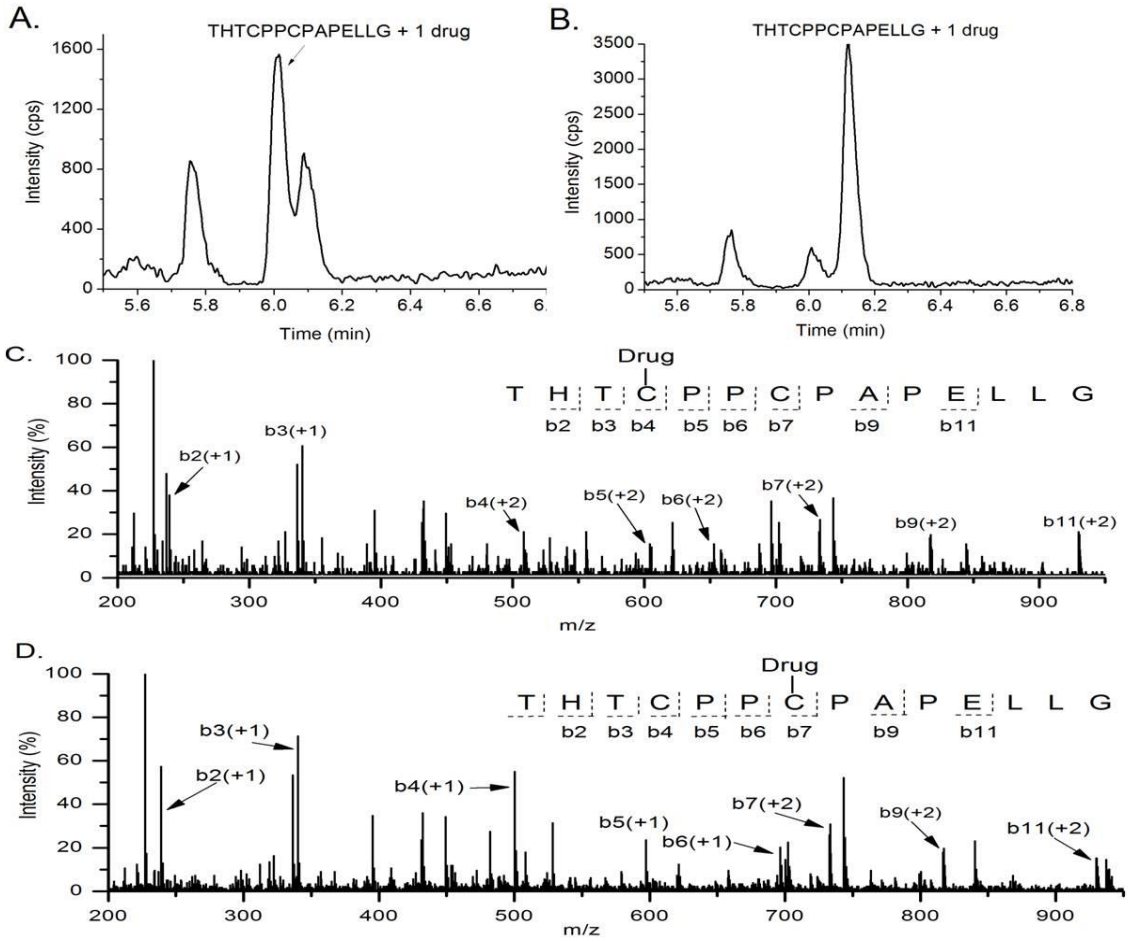

Figure 5. Identification of drug linking positions. A &B: Peak # 4 and #5 digests were detected with THTCPPCPAPELLG + 1 drug at 6.01 and 6.12 min, respectively. C: Fragmentation of RT= 6.01 min peak analyte. D) Fragmentation of RT=6.12 min peak analyte.

To determine the exact drug linking position, the two THTCPPCPAPELLG +1 drug ions detected at RT=6.01 and 6.12 min were fragmented and the b type ions were used to identify the drug linking positions. These two peptides shared same mass fragments of b1-b3 and b8-14, while with significant differences between b4-b7 due to the drug linking position variations.

Figure 5C demonstrated the fragments spectra of THTCPPCPAPELLG + 1 drug at RT=6.01 min. The detected m/z of 555.75, 604.28, 652.81, and 732.82Da matched well with the mass of b4 (+2), b5 (+2), b6 (+2) and b7 (+2) of the Cys_230 drug linked peptides, which confirmed drug linkage on Cys_230. Similarly, m/z of 500.17, 597.22, 694.28 and 732.86 Da were detected in the spectra of THTCPPCPAPELLG +1 drug at RT=6.12 min (Figure 5D). Those masses matched well with the b4 (+1), b5 (+1), b6 (+1) and b7 (+1) of the Cys_233 linked peptides and the drug was identified to be linked on Cys_233. Meanwhile, peak # 4 and #5 digests were also detected with SCDK +1 drug which proved the other drug linkage on Cys_224. The drug linking positions were summarized in Table 1.

Table 1. HC positional isomers drug linking positions.

Peak #	Number of drug	Drug linking position
#1	1	Cys_224
#2	1	Cys_230
#3	1	Cys_233
#4	2	Cys_224, Cys_230
#5	2	Cys_224, Cys_233
#6	2	Cys_230. Cys_233

3.5. DRUG DISTRIBUTION

Based on the subunit analysis and following by bottom up analysis. The drug distribution on LC and HC were calculated. Figure 6 demonstrated the processed data by combining the above stated analysis.

In the study, an abnormal phenomenon was observed in the hinge region Cys_230 and 233. The data showed that 50.3% of the HC had no drug conjugation at the hinge

region, 11.7% HC was linked with one drug on either Cys_230 or 233, and 38.0% of the HC was linked with 2 drugs at both of positions. It is quite abnormal that the percentage of one drug linkage is much lower than those of no drug linkage and 2 drugs linkage. Since the drug conjugation mainly depends on the reduction of the interchain disulfide bonds, the abnormal observation clearly indicates that the reduction of one pair of hinge region interchain disulfide favored the reduction of the other one. Similar phenomenon were observed in other interchain cysteine linked ADC[25, 26]. It was reported that the hinge region confirmation was changed for reduced monoclonal antibody due to the reduction of hinge region disulfide[28], which probably explained why this abnormal phenomenon was observed.

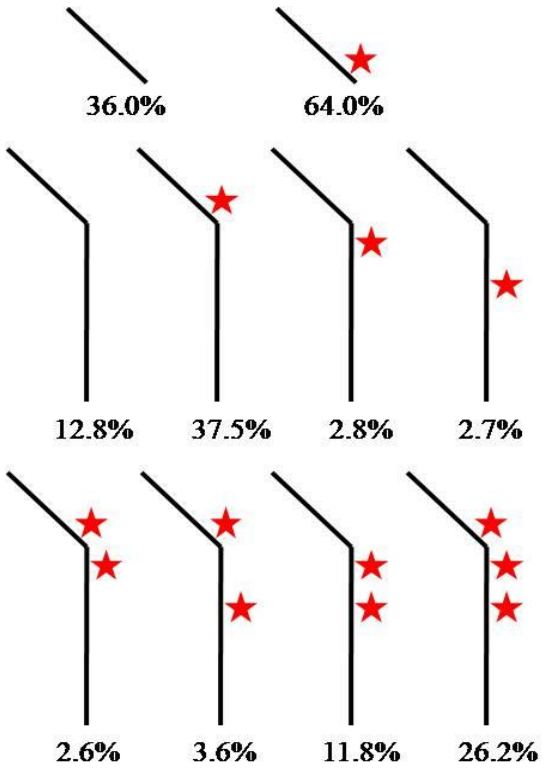

Figure 6. Drug distribution on light chains and heavy chains.

4. CONCLUSION

A novel mass spectrometry method was developed by combining subunit analysis and bottom up analysis for the characterization of the positional isomers of interchain cysteine linked ADCs. The subunit analysis provides effective way to evaluate the drug distribution on each chain, and the bottom up analysis using chymotrypsin digestion of IdeS treated ADCs produced relatively short peptides that preserved all the drug linking positions on the HC. The following LC/MS analysis separated those peptides and determined their relative abundances. The further MS/MS fragmentations of the analyte ions confirmed the drug linking positions. Overall, the positional isomers are well separated and their relative abundances was calculated. Since the method can provide accurate data on drug linking numbers and positions, it can be well used by researchers in ADC cancer drug discovery, development, and cancer treatment.

ACKNOWLEDGEMENT

The authors thank Mu Chen, Zhiling Zhang, Li Tan, Shengsheng Xu for their technical assistance and useful comments during the method development, and manuscript proof reading. This research was supported by Frontage laboratories, Inc. and Missouri University of Science and Technology.

REFERENCES

1. Ducry, L. and B. Stump, Antibody− drug conjugates: linking cytotoxic payloads to monoclonal antibodies. Bioconjugate chemistry, 2009. **21**(1): p. 5-13.

2. McCombs, J.R. and S.C. Owen, Antibody drug conjugates: design and selection of linker, payload and conjugation chemistry. The AAPS journal, 2015. **17**(2): p. 339-351.

3. Chari, R.V., M.L. Miller, and W.C. Widdison, Antibody–drug conjugates: an emerging concept in cancer therapy. Angewandte Chemie International Edition, 2014. **53**(15): p. 3796-3827.

4. Lambert, J.M. and C.Q. Morris, Antibody–drug conjugates (ADCs) for personalized treatment of solid tumors: a review. Advances in therapy, 2017. **34**(5): p. 1015-1035.

5. Beck, A., et al., Strategies and challenges for the next generation of antibody–drug conjugates. Nature Reviews Drug Discovery, 2017. **16**(5): p. 315.

6. Lambert, J.M. and A. Berkenblit, Antibody–drug conjugates for cancer treatment. Annual review of medicine, 2018. **69**: p. 191-207.

7. Jain, N., et al., Current ADC linker chemistry. Pharmaceutical research, 2015. **32**(11): p. 3526-3540.

8. Sun, M.M., et al., Reduction− alkylation strategies for the modification of specific monoclonal antibody disulfides. Bioconjugate chemistry, 2005. **16**(5): p. 1282-1290.

9. Lyon, R.P., et al., Conjugation of anticancer drugs through endogenous monoclonal antibody cysteine residues, in Methods in enzymology. 2012, Elsevier. p. 123-138.

10. Debaene, F.o., et al., Innovative native MS methodologies for antibody drug conjugate characterization: high resolution native MS and IM-MS for average DAR and DAR distribution assessment. Analytical chemistry, 2014. **86**(21): p. 10674-10683.

11. Valliere-Douglass, J.F., W.A. McFee, and O. Salas-Solano, Native intact mass determination of antibodies conjugated with monomethyl Auristatin E and F at interchain cysteine residues. Analytical chemistry, 2012. **84**(6): p. 2843-2849.

12. Xu, K., et al., Characterization of the drug-to-antibody ratio distribution for antibody–drug conjugates in plasma/serum. Bioanalysis, 2013. **5**(9): p. 1057-1071.

13. Li, Y., et al., A size exclusion-reversed phase two dimensional-liquid chromatography methodology for stability and small molecule related species in antibody drug conjugates. Journal of Chromatography A, 2015. **1393**: p. 81-88.

14. Chen, T., et al., Antibody-drug conjugate characterization by chromatographic and electrophoretic techniques. Journal of Chromatography B, 2016. **1032**: p. 39-50.

15. Thompson, P., et al., Rational design, biophysical and biological characterization of site-specific antibody-tubulysin conjugates with improved stability, efficacy and pharmacokinetics. Journal of controlled release, 2016. **236**: p. 100-116.

16. Guo, J., et al., Characterization and higher-order structure assessment of an interchain cysteine-based ADC: impact of drug loading and distribution on the mechanism of aggregation. Bioconjugate chemistry, 2016. **27**(3): p. 604-615.

17. Alley, S.C., et al., Contribution of linker stability to the activities of anticancer immunoconjugates. Bioconjugate chemistry, 2008. **19**(3): p. 759-765.

18. Shen, B.-Q., et al., Conjugation site modulates the in vivo stability and therapeutic activity of antibody-drug conjugates. Nature biotechnology, 2012. **30**(2): p. 184.

19. Baldwin, A.D. and K.L. Kiick, Tunable degradation of maleimide–thiol adducts in reducing environments. Bioconjugate chemistry, 2011. **22**(10): p. 1946-1953.

20. Valliere-Douglass, J.F., S.M. Hengel, and L.Y. Pan, Approaches to interchain cysteine-linked ADC characterization by mass spectrometry. Molecular pharmaceutics, 2014. **12**(6): p. 1774-1783.

21. Dosio, F., P. Brusa, and L. Cattel, Immunotoxins and anticancer drug conjugate assemblies: the role of the linkage between components. Toxins, 2011. **3**(7): p. 848-883.

22. Tumey, L.N., et al., Mild method for succinimide hydrolysis on ADCs: impact on ADC potency, stability, exposure, and efficacy. Bioconjugate chemistry, 2014. **25**(10): p. 1871-1880.

23. Birdsall, R.E., et al. A rapid on-line method for mass spectrometric confirmation of a cysteine-conjugated antibody-drug-conjugate structure using multidimensional chromatography. in MAbs. 2015. Taylor & Francis.

24. Le, L.N., et al., Profiling antibody drug conjugate positional isomers: a system-of-equations approach. Analytical chemistry, 2012. **84**(17): p. 7479-7486.

25. Janin-Bussat, M.-C., et al., Characterization of antibody drug conjugate positional isomers at cysteine residues by peptide mapping LC–MS analysis. Journal of Chromatography B, 2015. **981**: p. 9-13.

26. Wagner-Rousset, E., et al. Antibody-drug conjugate model fast characterization by LC-MS following IdeS proteolytic digestion. in MAbs. 2014. Taylor & Francis.

27. Liu, T., et al., Fast Characterization of Fc-Containing Proteins by Middle-Down Mass Spectrometry Following IdeS Digestion. Chromatographia, 2016. **79**(21-22): p. 1491-1505.

28. Pan, L.Y., O. Salas-Solano, and J.F. Valliere-Douglass, Conformation and dynamics of interchain cysteine-linked antibody-drug conjugates as revealed by hydrogen/deuterium exchange mass spectrometry. Analytical chemistry, 2014. **86**(5): p. 2657-2664.

II. ACCURATE DETERMINATION OF DRUG TO ANTIBODY RATIO OF INTERCHAIN CYSTEINE LINKED ANTIBODY DRUG CONJUGATES BY LC-HRMS

Ke Li[1], Zhiling Zhang[2], Zhongping (John) Lin[2], Honglan Shi[1], Yinfa Ma[1,3]*

[1]Department of Chemistry and Center for Biomedical Research, Missouri University of Science and Technology, Rolla, MO, 65409

[2]Department of Bioanalysis, Frontage Laboratories, Inc., Exton, PA, 19341

[3]Department of Chemistry, California State University, Sacramento, CA 95819

ABSTRACT

Accurate determination of drug to antibody ratio (DAR) of interchain cysteine linked antibody drug conjugates (ADCs) is challenging. High resolution mass spectrometry (HRMS) analysis of the ADCs at intact or subunit level provides a feasible way to measure the DAR. However, the determined DAR is usually lower than the real DAR because of the ionization efficiency variation between different DAR species. In this research, we developed novel standard free HRMS method involving isotope labeled payload conjugation, protease digestion and LC/HRMS analysis for the accurate determination of DAR of interchain cysteine linked ADCs with cleavable or non-cleavable linkers. Isotope labeled payload conjugation eliminated the structural and chemical difference between different DAR species and ensured the drugs or payload containing peptides separation in the mass spectrometer. Papain digestion strategy works for ADCs with cleavable linkers showed the determined DAR of 3.79 and relative standard deviation (% RSD) of 0.48 (n=3). Similarly, trypsin& chymotrypsin digestion strategy applicable to ADCs with non-

cleavable linkers showed determined DAR of 3.77 and %RSD of 0.86 (n=3). DAR determined by this method was consistent with DAR of the ADCs. This method will be very useful to researchers working in the field of ADCs discovery and development area.

Abstract Figure:

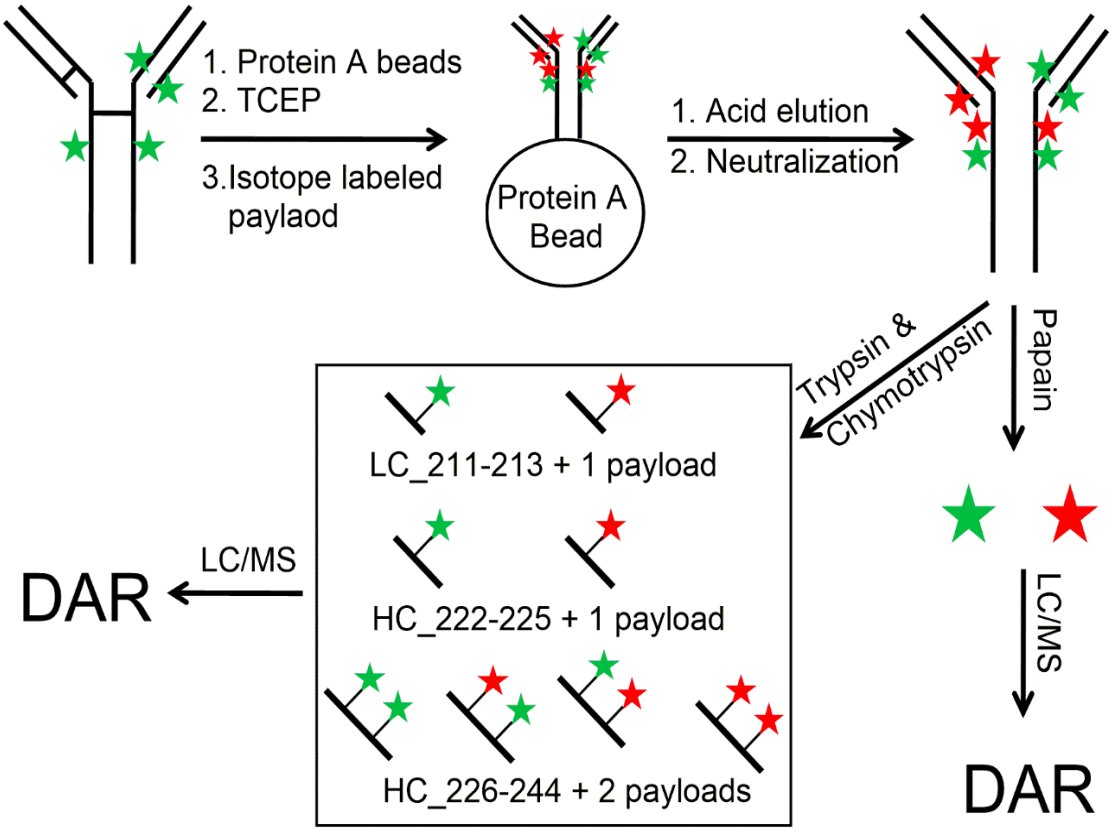

1. INTRODUCTION

Antibody drug conjugates (ADCs) are emerging therapeutic products specially designed for the treatment of Cancer. ADCs deliver the cytotoxic drugs to tumor cells

selectively and provide better therapeutic advantage for patients[1,2]. ADC consists three components: monoclonal antibody (mAb), stable linker, and cytotoxic drug. mAb has high specificity and affinity toward the targets on cancer cell surfaces and leads to drug accumulation on the tumor site while minimizing cross-reactivity with normal tissues[3]. Stable linker connect drug and antibody together via covalent bonds and possess strong stability during circulation[4,5].Cytotoxic drugs have potent toxicity even at very low concentrations and have high stability and sufficient solubility in the aqueous environment[6,7].After administration, the ADCs circulate in the body and diffuse to the tumor site, then they recognize and bind to the tumor-associated antigen expressed on the surfaces of cancer cells by its antibody component and form ADC/antigen complexes[8]which was internalized into the cancer cells through receptor-mediated endocytosis[9,10].Thereafter, the internalized ADCs are degraded in lysosome and the active drugs are released into the cytoplasm. The cytotoxic drugs usually induce DNA damage or cell cycle arrest and therefore trigger cell apoptosis[11].The high selectivity make ADCs promising anticancer drugs for treatment of cancers.

Among all the ADCs, interchain cysteine linked ADCs are the most popular one due to the controllable drug to antibody ratio (DAR) and heterogeneity[12]. It is estimated that approximate2/3 of all the ADCs under developing are interchain cysteine linked ADCs based on disclosed information[13].The interchain cysteine linked ADCs are manufactured by partial reduction of the 4 pairs of interchain disulfide bonds that are not critical for the structural stability while keeping the 12 intrachain disulfide bonds intact. The reduction generates 0-4 pairs of free thiols which are ready for conjugation with payloads (linker-drug). Conjugation of thiols with payloads containing maleimide linkers resulted

heterogeneous ADCs with DAR of 0, 2, 4, 6 and 8depending on the reduction condition of the interchain disulfide bonds[14,2].The DAR is an important parameter for the potential efficacy of ADCs and should be accurately determined[15].

Hydrophobic interaction chromatography (HIC)was often considered as gold standard for the analysis of the DAR of interchain cysteine linked ADCs[16], which was used to determine both the drug distribution and DAR. However, it required large amounts of ADCs (20 - 50 µg) and also required a high ADC concentration in samples. In recent years, high resolution mass (HRMS) analysis of ADCs at intact or subunit level provides a feasible way to determine the DAR[17-19].However, the DAR determined by the current HRMS methods is not accurate due to the ionization efficiency variation of different DAR species [17,20,21]. In HRMS analysis, the DAR was arbitrarily calculated based on the abundance of each species under the assumption that different DAR species have same ionization efficiencies[18].However, the ionization efficiency was naturally affected by the degree of hydrophobicity which was associated with the number of payload linked on the antibody[20]. It has been observed high DAR species has relatively lower ionization efficiency[17].Chen and coworkers compared the abundance of each DAR species measured by HRMS and HIC-UV/Vis method and found that HRMS method showed relatively low abundances of high DAR species comparing with HIC-UV/Vis results. Meanwhile, DAR of 2.9 determined HRMS was much lower than 3.4 determined by HIC method[17].

In this study, we developed novel HRMS methods for the accurate measurements of DAR. This method was standard free and require much less sample. Briefly, ADCs were captured on the protein A beads and were treated with tris (2-carboxyethyl) phosphine

(TCEP) to reduce the interchain disulfide bonds to free thiols. Thereafter, isotope labeled payloads were added to the beads suspension to alkylate the thiols. As a consequence, each antibody was linked with 8 payloads, either native or isotope labeled payloads. The ADCs were further digested with papain or trypsin& chymotrypsin mixture and the digests were analyzed by LC-HRMS. Free drugs or payload containing peptides were monitored to determine the DAR.

2. EXPERIMENTAL SECTION

2.1. RAGENTS AND MATERIALS

Papain, Sodium phosphate dibasic, Sodium phosphate monobasic, trifluoroacetic acid (TFA), urea, L-cysteine and 0.5 M EDTA (pH 8.0) were obtained from Sigma Aldrich (St. Louis, MO). Protein A magnetic beads (30mg/mL), 1 M tris (pH 7.4), 1 M tris (pH 8.0), TCEP and iodoacetamide were purchased from Thermo Fisher scientific (Rockford, IL).MC-VC-PAB-MMAE (vcMMAE) was purchased from Medkoo Biosciences (Morrisville, NC), trypsin and chymotrypsin were purchased from Promega corporation (Madison, WI),LC/MS grade acetonitrile (ACN),formic acid (FA)and LC/MS grade water were purchase from Fisher Scientific (Fair Lawn, NJ). Interchain cysteine linked ADCs employing NIST mAb and vcMMAE was synthesized in Frontage Laboratories (Exton, PA). DAR was determined to be DAR of 3.80 (See supplemental information). Isotope labeled payload (vcMMAE-d8) were provided by Frontage Laboratories (Exton, PA, See supplemental information for details).

2.2. INSTRUMENTAL CONDITIONS

Instrumental analysis was performed on LC/MS system employing Shimadzu LC30 for separation and AB Sciex 6600 QTOF for detection. Instrumental parameters were summarized in Table 1.

Table 1. Instrumental parameters of LC/MS

	LC/MS Method #1	LC/MS Method #2
LC setting		
Column	Waters Xbridge, Protein C4, 3.5 µm, 2.1×50 mm	Water Acquity BEH C18, 1.7 µm, 2.1×50 mm
Column Tempearture	Ambient	45 °C
Mobile phase A	0.1% formic acid in water	
Mobile phase B	0.1% formic acid in ACN	
Flow rate	0.3 mL/min	
Gradient	0-3 min: 5% B 3-3.5 min: 5% B-90% B 3.5-5.5 min 90% B 5.5-6 min 90% B-5% B 6-8 min 5% B	0-1 min 30% B 1-5 min 30% B-90% B 5-6.5min 90% B 6.5-7 min 90% B-30% B 7-9 min 30% B
MS setting		
Curtain Gas	25	
Ionization Source	ESI	
Temperature	500 °C	
Detection mode	Positive TOF MS	
IS voltage	5000 V	
Decluster potential	80	
Scan range	m/z: 500-4000	m/z: 100-2500
Dwell time	0.5 s	0.2 s
Bin size	40	4

2.3. VCMMAE-D8 CONJUGATION

ADCs solution containing 0.5 µg of ADCs was mixed with20µL of protein A magnetic beads (20 mg/mL), and then100 mM of TCEP solution was added to the beads

suspension to reach final TCEP concentration of 5.0mM. The beads suspension was incubated at room temperature for 30 min with agitation at 1000 rpm to prevent the beads precipitation. Thereafter, the beads were pulled down by using magnet and the supernatant was discarded. The beads were washed twice with conjugation buffer (50 mM phosphate, 2.5 mM EDTA, pH 7.0).

Prior conjugation, 50 µM of vcMMAE-d8 solution prepared in conjugation buffer was added to the beads. The beads suspension was incubated at 25℃ for 1 hr with agitation at 1000 rpm. While conjugation finishing, the beads were pulled down and the conjugation solution was discarded. The beads were washed with conjugation buffer twice and10% ACN once to remove the excessive vcMMAE-d8. Finally, the vcMMAE-d8 conjugated ADCs were eluted from the beads using 20 µL of 0.1% TFA in water and the eluted ADCs were neutralized with 2 µL of 1 M tris (pH 7.4).

2.4. SUBUNIT ANALYSIS

ADCs solution (before and after vcMMAE-d8 conjugation) were mixed with equal volume of 10 mM TCEP solution and the mixture was incubated for30 min. The subunit analysis was performed on a LC-HRMS system following LC/MS Method #1 as described in Instrumental conditions section. The raw mass spectra of the ADCs was processed with BioPharmaView software to obtain deconvoluted mass spectra.

2.5. PAPAIN DIGESTION ANALYSIS

Papain digestion was performed following manufacture’s protocol with minor modification. Briefly, papain solution containing 0.05 µg of papain was added to the eluted

ADC solution. L-cysteine was added to the mixture to5.0 mM. The mixture was incubated at 37°C for 60min.Thereafter, formic acid was added to the mixture to a final concentration of 0.5% to quench the digestion. ACN was also added to the solution to a final concentration of 20% prevent the precipitation of MMAE/MMAE-d8. The digests were analyzed by LC/MS following LC/MS Method #1. MMAE and MMAE-d8 were monitored to calculate DAR.

2.6. TRYPSIN & CHYMOTRYPSIN DIGESTION ANALYSIS

The eluted ADCs were denatured with 20 µL of 10 M urea in the presence of 5 mM TCEP at 37 °C for 1 hr. Then, iodoacetamide was added to 15 mM, and the mixture was incubated for 30 min in the dark. Prior digestion, digestion buffer containing 50 mM tris (pH 8.0) and 10% ACN was added to the mixture to dilute urea concentration to 1 M. Thereafter, 1 µg of trypsin and 0.1 µg of chymotrypsin were added to the mixture for digestion. The digestion was performed in a Rapid Enzyme Digestion System (400 W, 37°C) for 30min. Upon completion, formic acid was added to the mixture to a final concentration of 0.5% to quench the digestion. The digests were analyzed by LC/MS following LC/MS Method #2 as described in instrumental conditions section.

3. RESULTS AND DISCUSSION

3.1. VCMMAE-D8 CONJUGATION

To accurately measure the DAR, conjugation of isotope labeled payloads to the remaining interchain cysteine of the ADCs that don't have without native payload

conjugation is required. After isotope labeled payload conjugation, all different DAR species were transferred to DAR 8 species. Therefore, the structural physical and chemical differences between different DAR species were eliminated. Similarly, protease digestion efficiency variation between different DAR species in downstream protease digestion was also eliminated. While the mass differences between native and isotope labeled payloads made them still be able to be separated in mass spectrometer. Instead of using standard, isotope labeled payload conjugation provide a standard free way to determine the DAR. DAR may be determined by analyzing the percentage of native payload, which can be readily determined by bottom-up strategy taking the advantage of the same mass response factors of native and isotope labeled drugs as well as native and isotope labeled payload containing peptides.

To link vcMMAE-d8 to the remaining interchain cysteine, the ADCs were first reduced with 5 mM TCEP to fully reduce all remaining interchain disulfide bonds to free reactive sulfhydryl groups. Prior conjugation, buffer exchanged was performed to remove the excessive TCEP. vcMMAE-d8 was added to the reduced ADCs to conjugate the free sulfhydryl groups with vcMMAE-d8. As a result, each antibody was linked with 8 payloads, either vcMMAE or vcMMAE-d8. Figure 1A showed the deconvoluted mass spectra of the ADCs before vcMMAE conjugation. Light chain (LC) and LC +1 drug species were detected at 23,123 and 24,439 Da, respectively. Heavy chain (HC) with 0-3 drug species were detected with 4 peak clusters between 51-56 K Da due to the complexity of the glycan attachment. While after vcMMAE-d8 conjugation, only LC+1 drug and HC + 3 drugs species were detected (Figure 1 B). The missing of LC and HC with 0-2 drug species indicated that all the remaining interchain cysteines without drug linkages were

linked with vcMMAE-d8. In general, it was difficult to achieve complete conjugation for all reduced sulfhydryl groups due to the low substrate concentrations. However, protein A beads captured the all ADCs on the beads surface, which greatly enhanced the local ADCs concentrations and thus made it possible to reach complete conjugation within short time even though payload concentration was low.

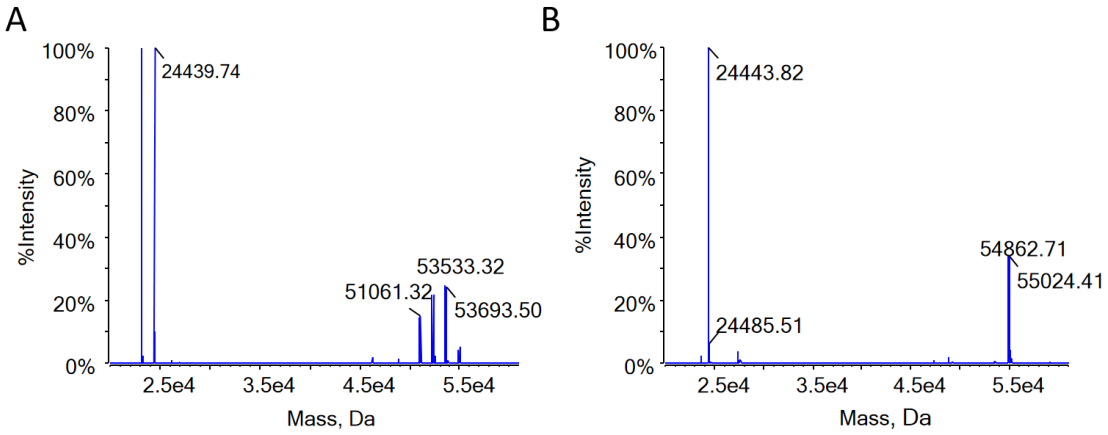

Figure 1. HRMS analysis of ADCs. A: Before isotope labeled payload conjugation. B: After isotope labeled payload conjugation.

A mass shifts of about 5 Da were observed for LC+1 payload after vcMMAE conjugation, and similar mass shift was also observed in HC +3 payloads species. Theoretically, LC + vcMMAE-d8 and LC+ vcMMAE had mass difference of 8 Da and there should had two peaks in deconvoluted mass spectra. However, majority of their raw mass spectra overlapped and QTOF was unable to differentiate those subtle differences. As a consequence, they were considered as one species by the mass spectrometer and were deconvoluted as one peak. The overlap and interaction of the two species resulted in an

enhanced mass spectra intensity between LC +vcMMAE and LC +vcMMAE-d8. Therefore, mass shift of about 5 Da was observed in the deconvoluted mass spectra.

3.2. DAR DETERMINATION BY PAPAIN DIGESTION

After isotope labeled payload conjugation, all the interchain cysteines were conjugated with either native or isotope labeled payloads. Then the ADCs were digested by papain in the presence of 5 mM cysteine. Papain effectively cleaved the linker at valine-citrulline position and led to the release of PAB-MMAE or PAB-MMAE-d8 which spontaneously eliminated PAB part and therefore generated free MMAE or MMAE-d8[113-114].The papain digests were analyzed by LC-HRMS system following optimized method. MMAE and MMAE-d8, as shown in Figure 2A, were detected at 4.45 min.

Table 2. DAR determination by papain digestion method.

Sample Name	Peak Area, 10^5 counts		Calculated DAR
	MMAE	MMAE-d8	
Sample #1	1.92	2.12	3.80
Sample #2	2.56	2.84	3.79
Sample #3	1.78	2.00	3.77
Avg.			3.79
%RSD			0.48

The chromatogram (Figure 2B) was extracted from the total ion chromatogram by using their first isotopic mass (781.45-718.65 for MMAE and 726.45-726.65 for MMAE-

d8). Their peak areas were summarized in Table 2 and DAR was calculated based on the following formula:

$$\mathrm{DAR} = \frac{\mathrm{Area}_{\mathrm{MMAE}}}{\mathrm{Area}_{\mathrm{MMAE}} + \mathrm{Area}_{\mathrm{MMAE-d8}}} \times 8$$

Papain digestion of isotope labeled payload conjugated ADCs provided a feasible and quick way to determine the DAR. DAR was determined to be 3.79 which were very consistent with the DAR of 3.80 determined by UV/Vis method. Meanwhile, this method showed great precision, the relative standard deviation (%RSD) was only 0.48%. Good accuracy and precision were obtained. While, it is worth to note that the papain digestion relies on the cleavability of linker, therefore itis only applicable to interchain cysteine linked ADCs with cleavable valine-citrulline linkers.

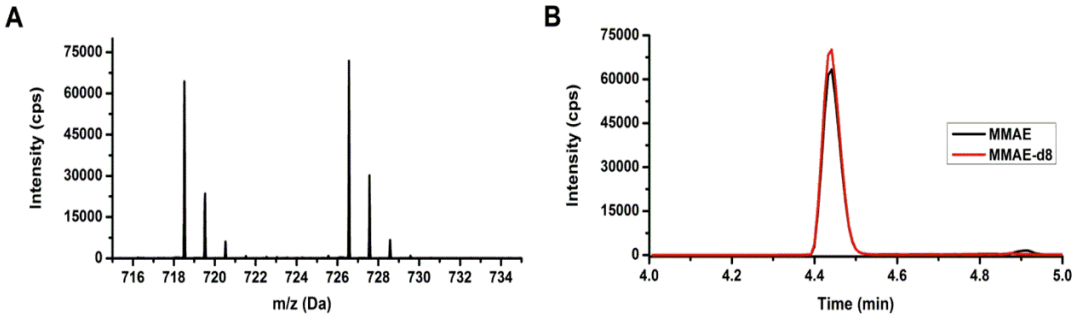

Figure 2. HPLC analysis of papain digest. A: Mass spectra of MMAE and MMAE-d8 from papain digest. B: Chromatogram of papain digest.

3.3. DAR DETERMINATION BY TRYPSIN & CHYMOTRYPSIN DIGESTION

Different with papain digestion, DAR determination by trypsin & chymotrypsin digestion requires determination of DAR contribution of each drug linking site. Interchain cysteine linked ADCs contain 4 drug linking site, one located on light chain and three

located on heavy chain. Trypsin & chymotrypsin digestion of ADCs resulted in three payload containing peptides: GEC (LC_211-213) with one payload linkage, SCDK (HC_222-225) with 1 payload linkage and THTCPPCPAPELLGGSVF (HC_226-244) with two payloads linkage. The digests were analyzed by LC-HRMS and all the payloads containing peptides were detected.

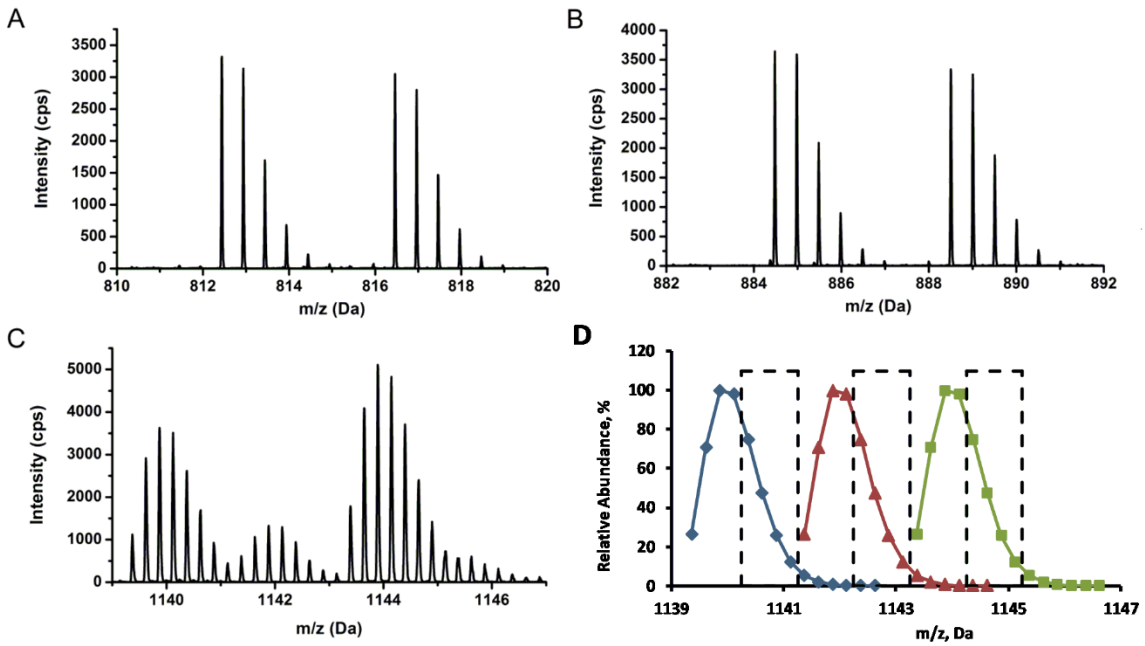

Figure 3. Mass spectra of payload containing peptides. A-C: Mass spectra of LC_211-213 + vcMMAE/vcMMAE-d8, HC_222-225 + vcMMAE/vcMMAE-d8 and HC_226-244 + 2 vcMMAE/vcMMAE-d8; D: Mass distribution of HC_226-244+ 2vcMMAE/vcMMAE-d8 species.

Figure 3A-Cdemonstrated the mass spectra of the payload-containing peptides. LC_211-213 + vcMMAE/vcMMAE-d8 was detected at 3.50minwith m/z of 812.44/816.46 Da (+2). Similarly, HC_222-225 + vcMMAE/vcMMAE-d8 was detected at 2.98 min with m/z of 884.48/888.50 Da. HC_226-244 has two payload linking sites, therefore, it may be

linked with two vcMMAE or vcMMAE + vcMMAE-d8 or two vcMMAE-d8. Those species were detected at 3.95 min with m/z of 1139.37, 1141.38 and 1143.39 Da (+4), respectively.

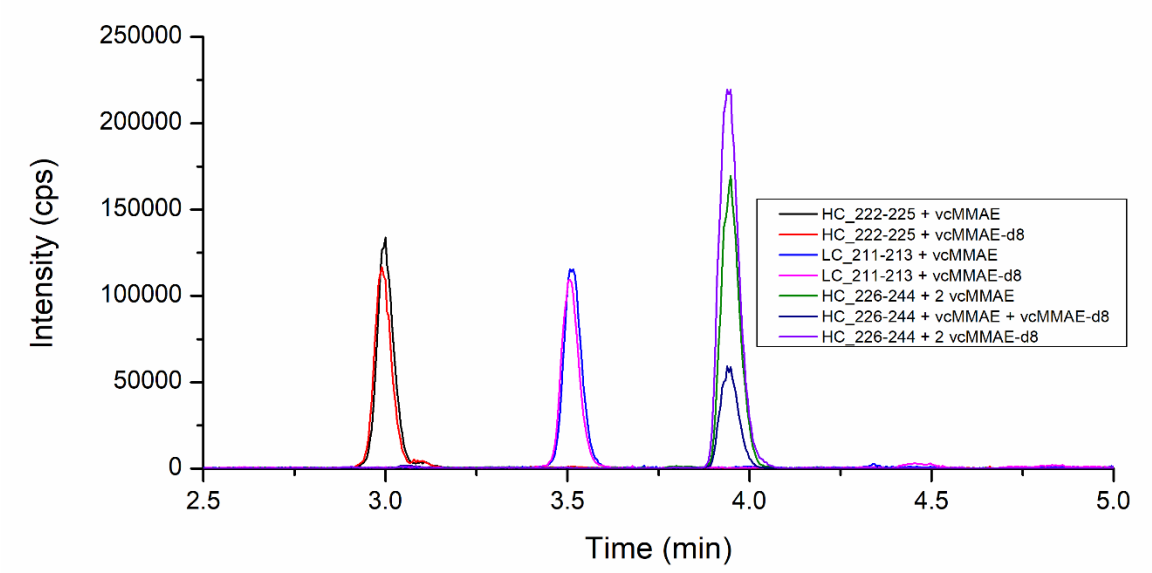

Figure 4. Chromatogram of trypsin & chymotrypsin digest.

The mass spectra of two short peptides were well separated. However, mass spectra overlap was observed in HC_222-244 + 2 vcMMAE/vcMMAE-d8 species (Figure 3C) due to their large molecular weight and relatively small mass differences. Mass spectra crosstalk apparently will impair the accuracy of results and therefore should be avoided while calculating DAR. The theoretical mass distributions (+4 state) of those species were plotted, as shown in Figure 4D, to determine the overlap condition of the mass spectra. The first four isotopic masses of each specie were observed with relative large mass crosstalk and therefore need to be avoided. The defined areas (dash line area) had very low crosstalk, less than 0.1%, and therefore was used for DAR determination.

Table 3. DAR determination by trypsin & chymotrypsin digestion method.

Sample Name	Peptide	Peak Area, 10^5 counts			DAR contribution	Calculated DAR
		MMAE-d8 #_0	MMAE-d8 #_1	MMAE-d8 #_2		
Sample #1	LC_211-213	3.30	3.02	NA	1.04	3.81
	HC_222-225	3.91	3.52	NA	1.05	
	HC_226-244	5.39	1.89	7.55	1.71	
Sample #2	LC_211-213	4.02	3.73	NA	1.04	3.77
	HC_222-225	4.31	3.99	NA	1.04	
	HC_226-244	6.03	2.10	8.56	1.70	
Sample #3	LC_211-213	3.04	2.84	NA	1.03	3.74
	HC_222-225	3.45	3.30	NA	1.02	
	HC_226-244	4.78	1.61	6.87	1.68	
Avg.						3.77
%RSD						0.86

The Chromatogram, as shown in Figure 4, was extracted from total ion chromatogram by first isotopic mass or defined range. The peak areas were summarized in Table 3. The DAR contribution of each site was calculated by following formula:

$$DAR = 2 \times \frac{A_{MMAE-d8\_1} + 2 \times A_{MMAE-d8\_2}}{A_{MMAE-d8\_0} + A_{MMAE-d8\_1} + 2 \times A_{MMAE-d8\_2}}$$

where:

AMMAE-d8_0=Peptide linked novcMMAE-d8 (only vcMMAE)

AMMAE-d8_1= Peptide linked 1 vcMMAE-d8

AMMAE-d8_2= Peptide linked 2 vcMMAE-d8

The overall DAR was calculated based on the DAR contribution of each site. Overall DAR was calculated to be 3.77 which was consistent with the DAR of 3.80 measured by UV/Vis method. The %RSD was determined to be 0.86%. Trypsin & chymotrypsin method demonstrated good accuracy and precision. Meanwhile, it is also

worth to mention that the DAR contributions of Cys_213 on light chain and Cys_223 (HC) on heavy chain were consistent, which also demonstrated the complete conjugation of isotope labeled drugs to remaining interchain cysteines that without native payload linkage.

In this study, we developed a novel standard free HRMS method for accurate determination of DAR of interchain cysteine linked ADCs. This method relied on combination of isotope labeled payload conjugation and protease digestion to determine the DAR and therefore should be also applicable to Thiomab cysteine linked antibody drug conjugates (TDCs) which are similar with interchain cysteine linked ADCs. In TDCs, the conjugation sites are specific and the payload linking mechanism is same as interchain cysteine linked ADCs, therefore it will also share all the advantages of this method. However, comparing with interchain cysteine linked ADCs, TDC are more simplified. TDCs only contain two drug linking positions. The standard is easy to obtain. Therefore, DAR determination by triple quadruple mass might be better regarding cost and detection limit.

Isotope labeled payload was an important part in this study. While preparing isotope labeled payload, the heavy isotopes may be incorporated in linker portion or drug portion. The isotope position has no impact on the ADCs with non-cleavable linkers because payload still remain intact after protease digestion. While, the heavy isotope position will significantly affect the ADCs with cleavable linkers. Incorporation of heavy isotopes in the linker portion will deactivate papain digestion method which relied on the drugs to determine the DAR. It’s obvious that incorporation of heavy isotope in drug portion have more advantages than in linker portion. While, it is worth to note that drug portion labeled

payload might be more expensive than linker portion labeled payload since considering the price of drug and linker.

In this study, bottom-up method was employed for determination of DAR after isotope labeled payload conjugation. It seemed middle-down analysis should be better than bottom-up method since the ionization efficiency variation between different DAR species were eliminated. However, the mass difference between native and isotope labeled payload was only 8 Da. While in deconvoluted mass spectra, LC and Fd peaks are quite wide, more than 20 Da. Obviously, 8 Da is not sufficient to guarantee separation of the native and isotope labeled payload linked species. Increase the mass difference between native and isotope labeled payload up to an extent of more than the peak width of LC and Fd might be a promising solution, but more costive should be expected.

4. CONCLUSION

Novel high-throughput mass methods were developed for the actually determination of the DAR of interchain cysteine linked ADC. The capture of ADCs on the protein A beads greatly enhanced the ADC concentration on the beads surface which made it possible for further conjugation. The conjugation of isotope labeled drug to the non-drug linking sites labeled the non-drug linkage site with isotope labeled drug. The latter subunit analysis of the isotope labeled drug conjugated ADC demonstrated the 1 drug linkage on light chain and 3 drug linkage on heavy chain proved completely conjugation to all the interchain cysteines. The labeled isotope drug not only eliminate the structural difference between each species but also guaranteed the non-identical digestion efficiency for each

species at the following protease digestion. The papain digestion cleaved the linker and generate free MMAE/MMAE-d8 can be directly used for the determination of the DAR. The trypsin & chymotrypsin digestion cleaved the long peptides to short peptides, the drug containing peptides are monitored for the determination of DAR. Meanwhile, complete digestion is not required since no chemical and structural difference between each species. The 8 Da difference between native drug and isotope labeled drug was large enough for the mass separation of free drug and drug containing peptides. More importantly, this method works for both cleavable and non-cleavable linkers and are standard free.

ACKNOWLEDGEMENTS

The authors gratefully acknowledge Dr. Mu Chen and Dr. Shengsheng Xu for technical assistance and useful discussions. We also thank Dr. Erhu Lu and Dr. Li Tan's suggestions on the synthesis of vcMMAE-d8. This study was supported by Frontage Laboratories, Inc. and Missouri University of Science and Technology.

CONFLICT OF INTEREST

Ke Li, Dr. Yinfa Ma and Dr. Honglan Shi were employees of Missouri University of Science and Technology at the time of this study, Dr. Zhiling Zhang and Dr. Zhongping (John) Lin were employees of Frontage Laboratories, Inc. This study was performed in Frontage Laboratories, Inc. The authors have no other relevant affiliations or financial involvement with any organization or entity with a financial interest in or financial conflict with the subject matter or materials discussed in the manuscript.

REFERENCES

1. Nasiri H, Valedkarimi Z, Aghebati- Maleki L, Majidi J (2018) Antibody- drug conjugates: Promising and efficient tools for targeted cancer therapy. Journal of cellular physiology 233 (9):6441-6457

2. Francisco JA, Cerveny CG, Meyer DL, Mixan BJ, Klussman K, Chace DF, Rejniak SX, Gordon KA, DeBlanc R, Toki BE (2003) cAC10-vcMMAE, an anti-CD30–monomethyl auristatin E conjugate with potent and selective antitumor activity. Blood 102 (4):1458-1465

3. Wang W, Wang E, Balthasar J (2008) Monoclonal antibody pharmacokinetics and pharmacodynamics. Clinical Pharmacology & Therapeutics 84 (5):548-558

4. Perez HL, Cardarelli PM, Deshpande S, Gangwar S, Schroeder GM, Vite GD, Borzilleri RM (2014) Antibody–drug conjugates: current status and future directions. Drug discovery today 19 (7):869-881

5. Teicher BA, Chari RV (2011) Antibody conjugate therapeutics: challenges and potential. Clinical cancer research 17 (20):6389-6397

6. Laguzza BC, Nichols CL, Briggs SL, Cullinan GJ, Johnson DA, Starling JJ, Baker AL, Bumol TF, Corvalan JR (1989) New antitumor monoclonal antibody-vinca conjugates LY203725 and related compounds: design, preparation, and representative in vivo activity. Journal of medicinal chemistry 32 (3):548-555

7. Pietersz G, Krauer K (1994) Antibody-targeted drugs for the therapy of cancer. Journal of drug targeting 2 (3):183-215

8. O'Mahony D, Bishop MR (2006) Monoclonal antibody therapy. Frontiers in bioscience: a journal and virtual library 11:1620-1635

9. Chari RV (2007) Targeted cancer therapy: conferring specificity to cytotoxic drugs. Accounts of chemical research 41 (1):98-107

10. Jaracz S, Chen J, Kuznetsova LV, Ojima I (2005) Recent advances in tumor-targeting anticancer drug conjugates. Bioorganic & medicinal chemistry 13 (17):5043-5054

11. Sievers EL, Senter PD (2013) Antibody-drug conjugates in cancer therapy. Annual review of medicine 64

12. Tsuchikama K, An Z (2018) Antibody-drug conjugates: recent advances in conjugation and linker chemistries. Protein & cell 9 (1):33-46

13. Jain N, Smith SW, Ghone S, Tomczuk B (2015) Current ADC linker chemistry. Pharmaceutical research 32 (11):3526-3540

14. Sanderson RJ, Hering MA, James SF, Sun MM, Doronina SO, Siadak AW, Senter PD, Wahl AF (2005) In vivo drug-linker stability of an anti-CD30 dipeptide-linked auristatin immunoconjugate. Clinical cancer research 11 (2):843-852

15. Schrama D, Reisfeld RA, Becker JC (2006) Antibody targeted drugs as cancer therapeutics. Nature reviews Drug discovery 5 (2):147

16. Ouyang J (2013) Drug-to-antibody ratio (DAR) and drug load distribution by hydrophobic interaction chromatography and reversed phase high-performance liquid chromatography. In: Antibody-Drug Conjugates. Springer, pp 275-283

17. Chen J, Yin S, Wu Y, Ouyang J (2013) Development of a native nanoelectrospray mass spectrometry method for determination of the drug-to-antibody ratio of antibody–drug conjugates. Analytical chemistry 85 (3):1699-1704

18. Valliere-Douglass JF, McFee WA, Salas-Solano O (2012) Native intact mass determination of antibodies conjugated with monomethyl Auristatin E and F at interchain cysteine residues. Analytical chemistry 84 (6):2843-2849

19. Debaene Fo, Bœuf A, Wagner-Rousset E, Colas O, Ayoub D, Corvaïa N, Van Dorsselaer A, Beck A, Cianférani S (2014) Innovative native MS methodologies for antibody drug conjugate characterization: high resolution native MS and IM-MS for average DAR and DAR distribution assessment. Analytical chemistry 86 (21):10674-10683

20. Wagh A, Song H, Zeng M, Tao L, Das TK Challenges and new frontiers in analytical characterization of antibody-drug conjugates. In: MAbs, 2018. vol 2. Taylor & Francis, pp 222-243

21. Friese OV, Smith JN, Brown PW, Rouse JC Practical approaches for overcoming challenges in heightened characterization of antibody-drug conjugates with new methodologies and ultrahigh-resolution mass spectrometry. In: MAbs, 2018. vol 3. Taylor & Francis, pp 335-345

22. Okeley NM, Miyamoto JB, Zhang X, Sanderson RJ, Benjamin DR, Sievers EL, Senter PD, Alley SC (2010) Intracellular activation of SGN-35, a potent anti-CD30 antibody-drug conjugate. Clinical Cancer Research 16 (3):888-897

23. Lu J, Jiang F, Lu A, Zhang G (2016) Linkers having a crucial role in antibody–drug conjugates. International journal of molecular sciences 17 (4):561

SUPPLEMENTARY INFORMATION

MC-VC-PAB-MMAE-D8 SYNTHESIS:

32 µL of 10mM MC-VC-PABC-PNP linker solution was mixed with 48 µL of 10 mM MMAE-d8, then HOBt and pyridine were added to final concentrations of 20µM and 50µM, respectively. The mixture was incubated at room temperature for 48hrs with agitation. Upon completion, 320µL of water was added to the mixture and then was loaded on a C18 column for separation, the MC-VC-PAB-MMAE-d8 fraction was collected and then lyophilized to a powder form. The powder was dissolved with 10µL of DMSO and future diluted to 50 µM with 50 mM of phosphate buffer (pH 7.0). Figure 1 displayed mass spectra and chromatogram of purified vcMMAE. vcMMAE was detected with m/z of 1324.7612 which was consistent with theoretical m/z of 1324.7865.

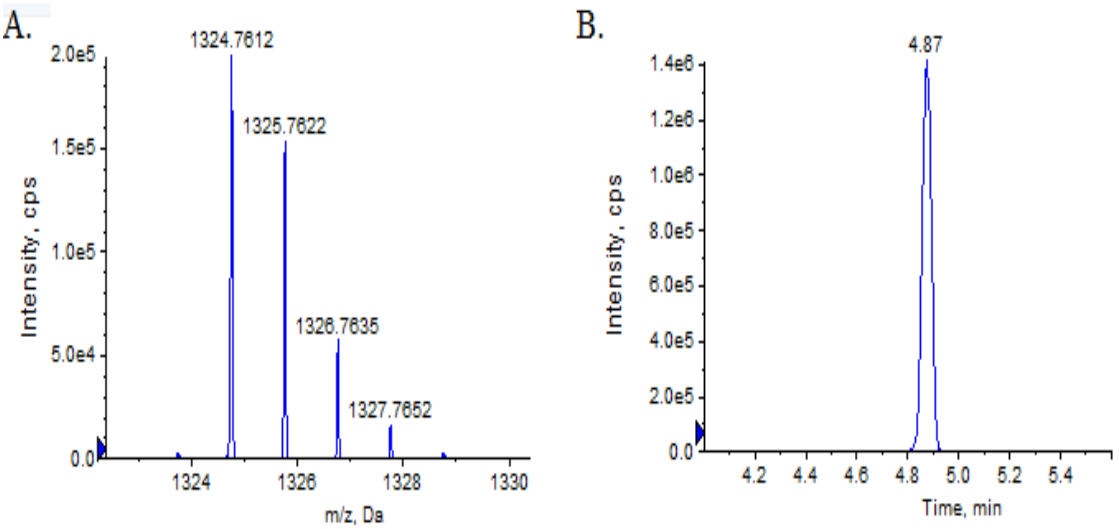

Figure 1. Purified vcMMAE-d8 confirmation. (A) Mass spectra of purified vcMMAE-d8. (B) Chromatogram of purified vcMMAE-d8.

ADC PREPARATION

500µg of antibody was dissolved in 100µL of PB-E (50mM phosphate, 2.5mM EDTA, pH7.0), contain 186 µM of TCEP and incubated under room temperature for 2 hr for reduction, afterwards, 100µL of 200µM MC-VC-PAB-MMAE prepared in PBE was added to the mixture and incubate for 1hr under RT. The synthesized ADCs were purified by passing through PD-10 desalting column to remove the excessive vcMMAE. The purified ADCs were lyophilized to dry and reconstituted to with PBS to 1 mg/mL.

DAR MEASUREMENT BY UV/VIS SPECTROMETRY

The DAR was measured by UV/Vis method. Briefly, the absorbance was measured at 248 nm and 280 nm. The DAR was calculated based on reported absorbance coefficient.

Table1. DAR measurement by UV/Vis method

	mAb		VC-MMAE	
	248 nm	280 nm	248 nm	280 nm
ε, $M^{-1}*cm^{-1}$	9.91E+04	2.11E+05	1.59E+04	1.50E+03

Test	Absorbance		A_{248}/A_{280}	DAR
	248 nm	280 nm		
#1	0.333	0.454	0.733	3.78
#2	0.341	0.462	0.738	3.85
#3	0.325	0.443	0.734	3.78
Average				3.80
%RSD				1.01

III. DESIGN, SYNTHESIS AND TOXICITY STUDY OF CETUXIMAB-STAUROSPORINE ON NON-SMALL CELL LUNG CANCERS

Ke Li[1], Zhiling Zhang[2], Zhongping (John) Lin[2], Honglan Shi[1], Yinfa Ma[1,3]*

[1]Department of Chemistry and Center for Biomedical Research, Missouri University of Science and Technology, Rolla, MO, 65409

[2]Department of Bioanalysis, Frontage Laboratories, Inc., Exton, PA, 19341

[3]Department of Chemistry, California State University, Sacramento, CA 95819

ABSTRACT

Non-small cell lung cancer is the major type of lung cancer that cause thousands of deaths each year. Most patients were diagnosed at later stages where chemotherapy was the dominant treatment therapy. However, chemotherapy had severe side effects and limited benefit on treatment due to its non-selectivity. Developing new drug to improve the selectivity of the drug was desired. Here we report the design and synthesis of new antibody drug conjugates for specially targeting of EGFR overexpressed the lung cancer. Cetuximab that has high affinity toward EGFR was selected as drug carrier, potent toxic Staurosporine was chosen as the cytotoxic agent to kill cells. A cleavable peptide linker was employed to link the Cetuximab and Staurosporine. The ADCs were successfully synthesized and the anticancer activity was evaluated on human A549 cells. Compared to Cetuximab, Cetuximab-Staurosporine showed significant toxicity toward A549 cells.

1. INTRODUCTION

Lung cancers is the leading causes of cancer related death in the United States. It is estimated about 220,000 of people are diagnosed with lung cancer and 158,000 patients die of it.[1] Non-small cell lung cancer (NSCLC) that accounts for 80% of the all the lung cancer patients was the major lung cancer type.[2] The two year survival rate is only 10%-20%.[3] For NSCLC, surgical resection that remove the tumor tissue was the desired therapy.[4] Unfortunately, most of the NSCLC patients were diagnosed at advanced stage where surgery was limited and chemotherapy became primary therapy. Chemotherapy employing non-selective toxic agent for treatment showed systemic toxicity to host and narrow therapeutic window.[5] Meanwhile, resistance was developed in many patients. Clearly, developing target therapies to overcome the drawbacks of chemotherapies was desired for the treatment of NSCLC.

Antibody-drug conjugates (ADCs) were an emerging target therapeutics specially designed for the treatment of cancer. Different with traditional drugs, ADCs were actually pro-drugs which have 3 components: monoclonal antibody (mAb), stable linker and potent cytotoxic anti-cancer agents. [6] The anti-cancer agents were conjugated the antibody via stable linkers. Monoclonal antibody specifically recognize the target expressed on tumor cell surface and bind to it. The following receptor mediated endocytosis internalized the ADCs into the cell where the anti-cancer agents were released to kill cancer cells from inside.[7] ADCs selectively deliver the anti-cancer agents to cancers cells and has none or low toxicity towards normal cells. It significantly expanded the therapeutic window

compared with the conventional chemotherapy and thus showed great promising on treatment of NSCLC.

EGFR is a tyrosine receptor on cell surface related with cellular proliferation regulation, differentiation, and cell survival. [8] It was reported one of the most significant oncogenes of cancer. [9] In NSCLC, EGFR was frequently overexpressed. Its aberrant expression induces abnormal abundant signaling transduction to the nucleus affecting cell cycle regulators, inflammatory agents and indirectly disorganizing the apoptotic pathway. [8] Overexpression of EGFR in NSCLC is correlated with a high metastatic rate, poor tumor differentiation, and a high rate of tumor growth [10]. In normal cells, the expression of EGFR was low. [11] While in some NSCLC, over expression of EGFR were detected. In a study, 70% specimens exhibited and 3+ EGFR staining in ICH assay. [12]. The big difference of EGFR expression makes EGFR a good target for developing of ADCs.

Cetuximab is an anti-EGFR mouse/human chimerical mAb developed for the treatment of cancer. It had been explored in the last decades on the treatment of NSCLC.[13] However, limited therapeutic advantage was observed mainly due to the acquired resistance. The reason involved in the mutation of the EGFR and the development of alternative signaling pathway by adapting to ERBB2 pathway.[14, 15] Dysregulation of EGFR internalization/degradation and subsequent EGFR-dependent activation of HER2 and HER3 was also reported as part of the reason.[16] Even though it showed limited therapeutic efficacy, it showed great affinity to the EGFR with Kd of 87 pM and strongly bind to EGFR despite the mutation.[17] Cetuximab was good mAb can specially target the NSCLC.

Staurosporine (STS), a potent toxic microbial alkaloid, was employed as anti-cancer agent to trigger cell death. It has high affinity to cyclin-dependent kinase 2 (CDK2) with IC 50 of 3.2 nM.[18] It binds to the ATP binding site and mimic the hydrogen bonds made by the adenine moiety of ATP.[19] Once bound, it forms hydrogen bonds with Glu-81, Leu-83, Asp-86 and Gln-131. The binding of STS to CDK2 forms a very hydrophobic environment and become inaccessible for the aqueous solvents which made it difficult for detachment of STS from CDK2.[20] Besides that, STS has high affinity to the PKCs and CDK2 with IC50 of 2.7 nM which are crucial for the cell survival.[21] Treatment of cells with STS induced the cell cycle arrested at G1/G2 phase and further induced apoptosis.[22] Staurosporine was a promising anti-cancer agent for the ADCs.

In this study, a new ADC (Cetuximab-STS) was designed to target NSCLC with EGFR over expression. Cetuximab was employed as carrier and STS was employed as anti-cancer agent to trigger cell death. A cleavable peptide linker was employed to link the cytotoxic Staurosporine to the Cetuximab. The ADCs were synthesized and characterized by HRMS. The anti-cancer activity was investigated on human lung cancer A549 cells.

2. EXPERIMENTAL SECTION

2.1. REAGENTS AND MATERIALS

Sodium phosphate dibasic, Sodium phosphate monobasic and 0.5 M EDTA (ph 8.0), PBS, cell Counting kit (WST-8), Hydroxybenzotriazole (HOBt) and pyridine were obtained from Sigma Aldrich (St. Louis, MO). Cetuximab was purchased from Selleck Chemical (Houston, TX). Maleimidocaproyl-L-valine-L-citrulline-p-aminobenzyl alcohol

p-nitrophenyl carbonate (MC-VC-PABC-PNP) and staurosporine were obtained from MedChemExpress LLC (Monmouth Junction, NJ). A549 cells, F12-K medium, Fatal bovine serum, Penicillin-Streptomycin Solution, 0.025% trypsin solution were purchased from ATCC (Manassas, VA), 1 M tris (pH 7.4), 1 M tris (pH 8.0), tris(2-carboxyethyl)phosphine (TCEP) were purchased from Thermo Fisher scientific (Rockford, IL). LC-MS grade acetonitrile (ACN), formic acid and water were purchase from Fisher Scientific (Fair Lawn, NJ). PD 10 desalting column was purchased from GE Healthcare Life Science (Pittsburgh, PA)

2.2. SYNTHESIS OF VCSTS

MC-VC-PABC-PNP and staurosporine were dissolved in DMF at final concentration of 5mM and 7.5 mM, respectively. HOBt and pyridine were added to the mixture to final concentration of 20 µM and 50 µM. The mixture was incubated at room temperature for 48 hr with agitation. Upon finish, the mixture was loaded on a C18 column, water and ACN was used as mobile phase for the separation. The vcSTS fraction was collected and lyophilized to dry. The vcSTS was dissolved in DMSO to get final concentration of 1 mM.

2.3. CETUXIMAB-STS SYNTHESIS

1 mg of Cetuximab solution was mixed with 5 mL of protein A beads (30 mg/mL) and incubated for 30 min with agitation. TCEP was added to the mixture to final concentration of 0.1 mM and keep incubate for 30 min. The beads were pull down with magnet and washed with conjugation buffer (50 mM phosphate, 10% ACN, pH 7.4) twice

to remove the excessive TCEP. The beads were suspended in 5 mL of conjugation buffer. vcSTS was added to the beads suspension to a final concentration of 15 µM. The beads suspension was incubated at RT for 1 hr with agitation. While finish, the beads were pull down with magnet and washed three times with conjugation buffer. The ADCs were eluted from beads by 2.5 mL of 10 mM phosphate buffer (pH 2.8). The eluted ADCs were passed through a PD 10 desalting column equilibrated with 10 mM of phosphate buffer (pH 7.0). The ADCs solution was filtered through 0.22 µm PVDF filter under sterile condition and store in sterile container.

2.4. CETUXIMAB-STS CHARACTERIZATION

To reduce the heterogeneity, 10 µg ADCs were mixed with 10 unit of IdeS and the mixture was incubated at 37 °C for 1 hr. TCEP was added to the mixture to final concentration of 5 mM and incubate at RT for 30 min. Afterwards, equal volume of 20% ACN in 50 mM tris (pH 7.4) was added to the mixture. The DAR analysis was performed on LC-QTOF system with water containing 0.1% formic acid as mobile phase A and ACN containing 0.1% formic acid as mobile phase B. The digest was loaded on a C4 column (Waters BEH Protein, C4, 3.5 µm, 2.1 x 100 mm, 300 angstroms), a 2 min isocratic elution with 5% mobile phase was applied for online desalting. The analytes were eluted from the column by increase the % B to 75% within 0.5 min and kept at 75% B for another 2 min. A Sciex 6600 QTOF mass spectrometer was coupled with the LC system for data acquisition. The mass spectrometer was operated in positive mode with mass range of m/z of 800-4000. The accumulation time was set at 0.5 seconds; bin size was set at 20. The

native mass spectra of the analytes was process with BioPharmaView software to obtain deconvolution mass spectra.

2.5. CELL CULTURE

A549 cells were cultured in F12-K medium containing 10% fetal bovine serum and antibiotic–antimycotic agent at 37 °C in a humidified incubator with 5% CO2/air. Cells were trypsinized and harvested at 90% confluence. Cells were suspended in medium for further assay.

2.6. CELL VIABILITY ASSAY

A549 cells were inoculated in 96 well plate at 5 × 104 cells/well in F12-K medium. The supernatant was removed after incubation at 37 °C and 5% CO2 for 24 hr. 100 μL of Cetuximab/Cetuximab-STS solution prepared in F12K medium at 0, 1 nM, 5 nM, 10 nM, 0.25 nM, 0.5 nM and 1 nM were added to the wells. The cells were incubated at 37°C in 5% CO2 for 72 hr. After Cetuximab/Cetuximab-STS treatment, 10 μL of WST-8 solution was added into each well and mixed well. The cells were incubated at 37°C for 45 min. After incubation, the absorbance (A) at $\lambda = 460$ nm was read on a plate reader.

3. RESULTS AND DISCUSSION

3.1. SYNTHESIS OF VCSTS

After 48 hr reaction, vcSTS, as shown in Figure 1, was successfully synthesized. vcSTS was purified by LC and pure vcSTS was obtained. The synthesized vcSTS was characterized by LC-HRMS to make sure the. The mass was detected at 1065.5 Da, which

matched well with theoretical mass. Meanwhile, the compound was fragmented under CID mode. The fragments were matched well with the theoretical mass as shown in Figure 1.

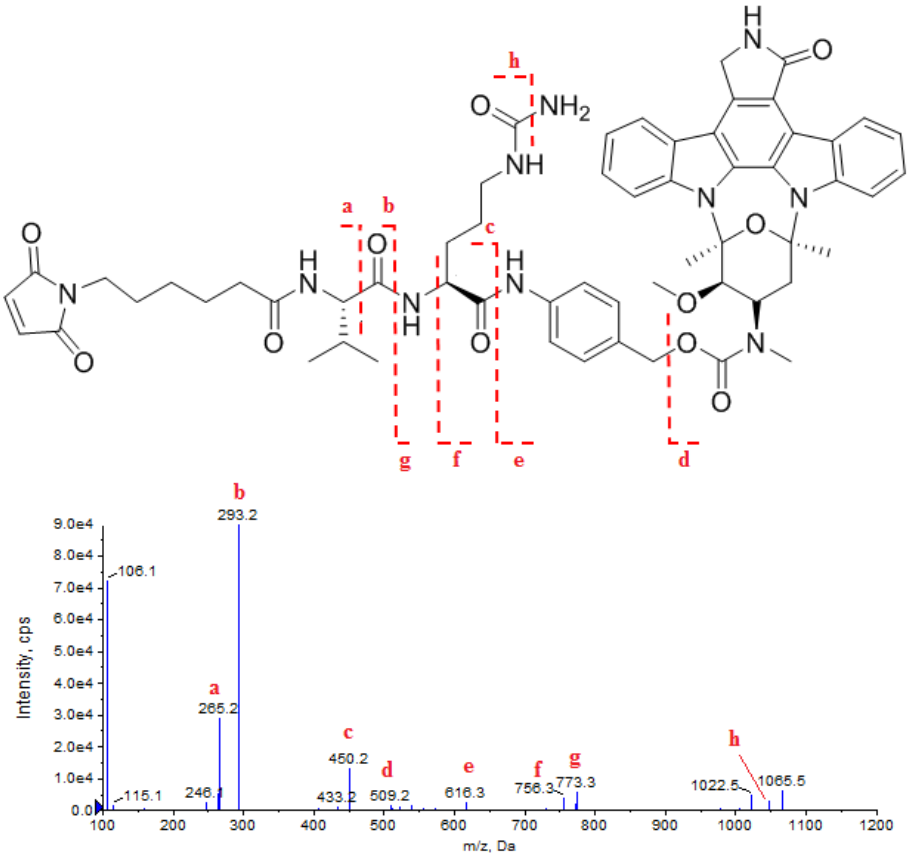

Figure 1. Structure of vcSTS and MS characterization of vc STS.

3.2. CETUXIMAB-STS CHARACTERIZATION

Cetuximab-STS was a heterogeneous mixture showed greatly complexity. Cetuximab has 4 glycosylation located on heavy chain. Two of them located on the Fc (Asn_297), the other two located on the Fd (Asn_88). The great difference on the glycan forms plus the drug linking number difference made it challenging for the drug to antibody ratio determination. Native LC-HRMS analysis at intact level is difficult because the

difficulties on the interpretation of the mass spectra. Deglycoyslation by PNGase F successfully removed the glycan attached on Fc under native condition. However, the glycan on the Fd was not removed under native condition (See supplemental information) which probably due to the position hindrance made it inaccessible to the enzyme. While the complexity of the glycan on the Fd still made it difficult to interpret the mass spectra.

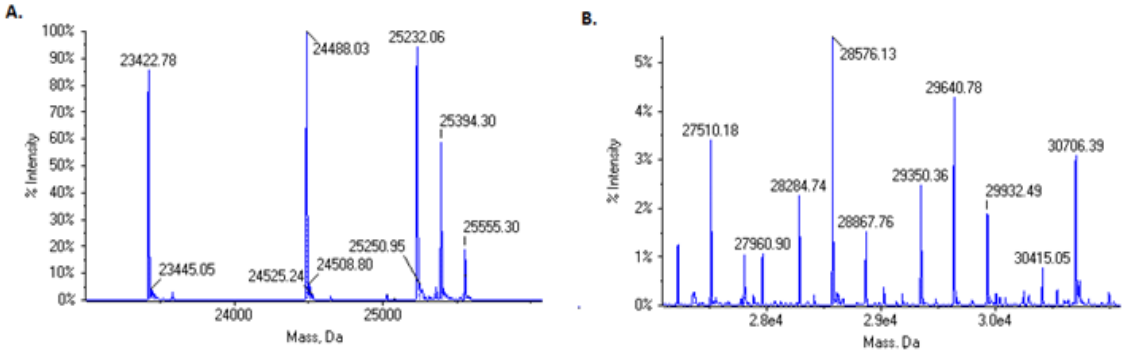

Figure 2. Characterization of Cetuximab-STS. A: Deconvoluted mass spectra of light chain and Fc species. B: Deconvoluted mass spectra of Fd species.

Instead of analyze ADCs at intact level, IdeS treatment of the ADCs successfully cleaved the ADCs at hinge region and thus removed the Fc portion and reduced the heterogeneity. The further treatment of TCEP reduced the interchain disulfide bonds and generated LC and Fd species that carrying all the drugs was subjected for LC-HRMS analysis. Figure 2A showed the deconvolution mass spectra of the ADCs fragments. The light chain species were detected at 23424 Da and 24488 Da, with mass difference of 1064 Da which matched well with the MW of the vcSTS. Fcs were detected with three major forms with MW of 25232, 25394 and 25555 Da with mass shift of 1443, 1605 and 1766 Da of deglycosylated Fc (MW: 23789 Da, See supplemental information). These shift

matched well with the mass of G0F, G1F and G2F. Fd species were detected with peak clusters between 27 KDa and 31KDa. Fd species showed complicated mass spectra due to the glycan on the Asn_88 (Figure 2B). Three major and four minor form of Fds were detected. However, due to the low abundance of the four minor forms, the DAR was estimated by three major forms. Table 1 displayed the deconvolution DAR calculation of the ADCs. The DAR was estimated to be 4.0.

Table 1. DAR calculation by HRMS.

Name	Observed MW, Da	Reconstruction Peak Area		Percentage,%	DAR Contribution
Fd	27219	26659	111051	19%	0
	27510	59896			
	27803	24496			
Fd + 1 drug	28285	44460	184363	31%	0.62
	28576	108179			
	28868	31725			
Fd + 2 drugs	29350	56814	188551	32%	1.28
	29641	84469			
	29932	47269			
Fd + 3 drugs	30415	14357	106362	18%	1.08
	30706	84606			
	30996	7400			
LC	23423	1765877	3761118	47%	0
LC + 1 drug	24488	1995241		53%	1.06
DAR					4.04

3.3. CETUXIMAB-STS TOXICITY

The toxicity of Cetuximab-STS was investigated on A549 cell which has moderate EGFR expression. Cetuximab was used as positive controls. The Cetuximab and Cetuximab-STS was prepared in cell culture media at concentration of 0.0334, 0.0667, 0.2, 0.667 and 1.000 μM. The toxicity data as shown in Figure 3.

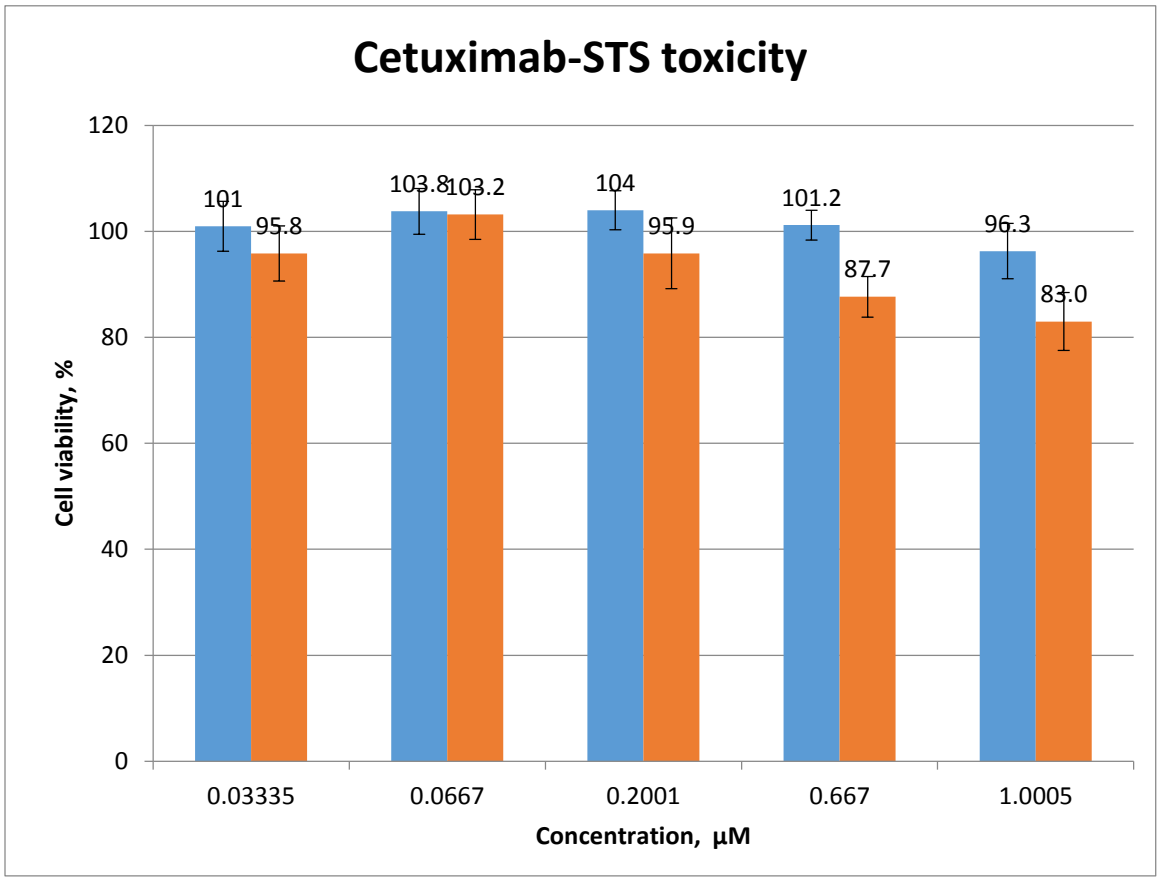

Figure 3. Toxicity of Cetuximab and Cetuximab-Staurosporine to A549 cells.

Within the test range, Cetuximab didn't show significant toxicity towards A549 cells, which was consistent with published data. Cetuximab-STS didn't show toxicity towards A549 cells at lower concentration. Its toxicity increased along with the increase of the ADCs dose concentration. At higher concentration, Cetuximab-STS significant induced toxicity to the A549 cells at 0.667 and 1 µM comparing with Cetuximab. Higher concentration supposed to have higher toxicity, however, higher concentration tends to aggregate probably due to the high hydrophobicity of the payload which has poor solubility in aqueous phase. So, the EC50 was calculated to be 2.6 µM based on the toxicity data.

4. CONCLUSION

Cetuximab –Staurosporine, a new ADC targeting EGFR, was successfully designed and synthesized. A cleavable linker was employed to link the Staurosporine and Cetuximab. Instead of using in solution conjugation, on beads conjugation method was employed for the manufacture of ADCs. vcSTS was very hydrophobic and therefore had very poor solubility in aqueous phase. Its solubility is less than 10 μM which made it difficult for conjugation. Protein A beads captured the antibodies on the surfaces of the beads and the concentration of antibodies at the surface of beads was greatly enhanced. As a consequence, the conjugation finished within 1 hour despite the low concentration of payload. Cetuximab contains 4 glycans and two of the glycans on the Fab were resistant to the PNGase F digestion probably due to the structural hindrance. Therefore, the synthesized ADCs were characterized by middle down strategy considering the complexity of the glycan. All the fragments were detected, and the DAR was calculated to be 4.0 based on the abundance of each species. The anticancer toxicity of Cetuximab-Staurosporine was evaluated on human A549 cells which had moderate expression of EGFR. Cetuximab was used as positive control. Comparing with Cetuximab, Cetuximab showed significant toxicity toward A549 cells. The EC 50 was calculated to be 2.6 μM. The EC50 was relatively high probably due to the high hydrophobicity induced by the payload. The ADCs might aggregate and lower the anticancer effectiveness. In summary, Cetuximab-Staurosporine was successfully synthesized and significant anticancer toxicity was observed. Further optimize the DAR should achieve better anticancer effectiveness.

ACKNOWLEDGEMENTS

The authors thank Mu Chen, Zhiling Zhang, Li Tan, Shengsheng Xu for their technical assistance, useful comments during the method development, and manuscript proof reading. This research was supported by Frontage laboratories, Inc and Missouri University of Science and Technology.

REFERENCES

1. Siegel, R.L., K.D. Miller, and A. Jemal, Cancer statistics, 2016. CA: a cancer journal for clinicians, 2016. 66(1): p. 7-30.

2. Torre, L.A., et al., Global cancer statistics, 2012. CA: a cancer journal for clinicians, 2015. 65(2): p. 87-108.

3. Schiller, J.H., et al., Comparison of four chemotherapy regimens for advanced non–small-cell lung cancer. New England Journal of Medicine, 2002. 346(2): p. 92-98.

4. Beland, M.D., et al., Primary non–small cell lung cancer: review of frequency, location, and time of recurrence after radiofrequency ablation. Radiology, 2009. 254(1): p. 301-307.

5. Chari, R.V., M.L. Miller, and W.C. Widdison, Antibody–drug conjugates: an emerging concept in cancer therapy. Angewandte Chemie International Edition, 2014. 53(15): p. 3796-3827.

6. Ducry, L. and B. Stump, Antibody− drug conjugates: linking cytotoxic payloads to monoclonal antibodies. Bioconjugate chemistry, 2009. 21(1): p. 5-13.

7. Sievers, E.L. and P.D. Senter, Antibody-drug conjugates in cancer therapy. Annual review of medicine, 2013. 64.

8. Tsiambas, E., et al., EGFR gene deregulation mechanisms in lung adenocarcinoma: A molecular review. Pathology-Research and Practice, 2016. 212(8): p. 672-677.

9. Bublil, E.M. and Y. Yarden, The EGF receptor family: spearheading a merger of signaling and therapeutics. Current opinion in cell biology, 2007. 19(2): p. 124-134.

10. Pavelic, K., et al., Evidence for a role of EGF receptor in the progression of human lung carcinoma. Anticancer research, 1993. 13(4): p. 1133-1137.

11. Carpenter, G. and S. Cohen, Epidermal growth factor. Annual review of biochemistry, 1979. 48(1): p. 193-216.

12. Mukohara, T., et al., Expression of epidermal growth factor receptor (EGFR) and downstream-activated peptides in surgically excised non-small-cell lung cancer (NSCLC). Lung cancer, 2003. 41(2): p. 123-130.

13. Hanna, N., et al., Phase II trial of cetuximab in patients with previously treated non–small-cell lung cancer. Journal of Clinical Oncology, 2006. 24(33): p. 5253-5258.

14. Yonesaka, K., et al., Activation of ERBB2 signaling causes resistance to the EGFR-directed therapeutic antibody cetuximab. Science translational medicine, 2011. 3(99): p. 99ra86-99ra86.

15. Bardelli, A. and S. Siena, Molecular mechanisms of resistance to cetuximab and panitumumab in colorectal cancer. Journal of clinical oncology, 2010. 28(7): p. 1254-1261.

16. Wheeler, D.L., et al., Mechanisms of acquired resistance to cetuximab: role of HER (ErbB) family members. Oncogene, 2008. 27(28): p. 3944.

17. Patel, D., et al., IgG isotype, glycosylation, and EGFR expression determine the induction of antibody-dependent cellular cytotoxicity in vitro by cetuximab. Human antibodies, 2010. 19(4): p. 89-99.

18. Rialet, V. and L. Meijer, A new screening test for antimitotic compounds using the universal M phase-specific protein kinase, p34cdc2/cyclin Bcdc13, affinity-immobilized on p13suc1-coated microtitration plates. Anticancer research, 1991. 11(4): p. 1581-1590.

19. Toledo, L.M. and N.B. Lydon, Structures of staurosporine bound to CDK2 and cAPK–new tools for structure-based design of protein kinase inhibitors. Structure, 1997. 5(12): p. 1551-1556.

20. Lawrie, A.M., et al., Protein kinase inhibition by staurosporine revealed in details of the molecular interaction with CDK2. Nature structural biology, 1997. 4(10): p. 796-801.

21. Tamaoki, T., et al., Staurosporine, a potent inhibitor of phospholipidCa++ dependent protein kinase. Biochemical and biophysical research communications, 1986. 135(2): p. 397-402.

22. Courage, C., R. Snowden, and A. Gescher, Differential effects of staurosporine analogues on cell cycle, growth and viability in A549 cells. British journal of cancer, 1996. 74(8): p. 1199.

SECTION

2. CONCLUSIONS

In this work, novel high resolution mass spectrometry method was developed for the characterization of heterogeneity of the interchain cysteine linked ADCs. In HRMS analysis of the reduced subunit of the ADCs, all the subunits were detected, therefore it provided the overall drug distribution information. Latter bottom up strategy was employed to determine the positional isomer distribution as well as to identify the drug linking positons. ADC were well characterized by combining subunit analysis and bottom up analysis.

In addition, novel method was also developed to accurately determine the DAR. Isotope labeled payload conjugation of the remaining interchain cysteines transferred different DAR species to DAR 8 species. Therefore, variations of the ionization efficiency and downstream protease digestion were eliminated. Papain or trypsin & chymotrypsin digestion provided feasible ways to determine the DAR of interchain cysteine linked ADCs with cleavable and non-cleavable linkers. The results matched well with the DAR determined by standard method. Good accuracy and precision was achieved.

In the last part of the research, Cetuximab was designed and successfully synthesized employing Cetuximab as drug carrier and Staurosporine as cytotoxic agents. The Synthesized ADCs were characterized by HRMS. The DAR of the ADCs was determined and the anticancer effect was evaluated on A549 cells. The results indicated significant toxicity of Cetuximab-Staurosporine toward A549 cells.

BIBLIOGRAPHY

1. Siegel, R. L.; Miller, K. D.; Jemal, A., Cancer statistics, 2019. CA: a cancer journal for clinicians 2019, 69 (1), 7-34.

2. Cheung-Ong, K.; Giaever, G.; Nislow, C., DNA-damaging agents in cancer chemotherapy: serendipity and chemical biology. Chemistry & biology 2013, 20 (5), 648-659.

3. Chen, H.; Lin, Z.; Arnst, K. E.; Miller, D. D.; Li, W., Tubulin inhibitor-based antibody-drug conjugates for cancer therapy. Molecules 2017, 22 (8), 1281.

4. Purcell, W. T.; Ettinger, D. S., Novel antifolate drugs. Current oncology reports 2003, 5 (2), 114-125.

5. Haag, R.; Kratz, F., Polymer therapeutics: concepts and applications. Angewandte Chemie International Edition 2006, 45 (8), 1198-1215.

6. Lambert, J. M.; Morris, C. Q., Antibody–drug conjugates (ADCs) for personalized treatment of solid tumors: a review. Advances in therapy 2017, 34 (5), 1015-1035.

7. Ford, C.; Newman, C.; Johnson, J.; Woodhouse, C.; Reeder, T.; Rowland, G.; Simmonds, R., Localisation and toxicity study of a vindesine-anti-CEA conjugate in patients with advanced cancer. British journal of cancer 1983, 47 (1), 35.

8. Firer, M. A.; Gellerman, G., Targeted drug delivery for cancer therapy: the other side of antibodies. Journal of hematology & oncology 2012, 5 (1), 70.

9. Ducry, L.; Stump, B., Antibody− drug conjugates: linking cytotoxic payloads to monoclonal antibodies. Bioconjugate chemistry 2009, 21 (1), 5-13.

10. Casi, G.; Neri, D., Antibody–Drug Conjugates and Small Molecule–Drug Conjugates: Opportunities and Challenges for the Development of Selective Anticancer Cytotoxic Agents: Miniperspective. Journal of medicinal chemistry 2015, 58 (22), 8751-8761.

11. Nasiri, H.; Valedkarimi, Z.; Aghebati- Maleki, L.; Majidi, J., Antibody- drug conjugates: Promising and efficient tools for targeted cancer therapy. Journal of cellular physiology 2018, 233 (9), 6441-6457.

12. Maverakis, E.; Kim, K.; Shimoda, M.; Gershwin, M. E.; Patel, F.; Wilken, R.; Raychaudhuri, S.; Ruhaak, L. R.; Lebrilla, C. B., Glycans in the immune system and the Altered Glycan Theory of Autoimmunity: a critical review. Journal of autoimmunity 2015, 57, 1-13.

13. Hughes, B., Antibody–drug conjugates for cancer: poised to deliver? Nature Publishing Group: 2010.

14. Chari, R. V.; Miller, M. L.; Widdison, W. C., Antibody–drug conjugates: an emerging concept in cancer therapy. Angewandte Chemie International Edition 2014, 53 (15), 3796-3827.

15. Teicher, B. A.; Chari, R. V., Antibody conjugate therapeutics: challenges and potential. Clinical cancer research 2011, 17 (20), 6389-6397.

16. Singh, R.; Lambert, J. M.; Chari, R. V., Antibody- Drug Conjugates: New Frontier in Cancer Therapeutics. Handbook of therapeutic antibodies 2014, 341-362.

17. Lambert, J. M., Typical antibody–drug conjugates. Antibody- Drug Conjugates: Fundamentals, Drug Development, and Clinical Outcomes to Target Cancer 2016, 1-32.

18. Singh, R.; Setiady, Y. Y.; Ponte, J.; Kovtun, Y. V.; Lai, K. C.; Hong, E. E.; Fishkin, N.; Dong, L.; Jones, G. E.; Coccia, J. A., A new triglycyl peptide linker for antibody–drug conjugates (ADCs) with improved targeted killing of cancer cells. Molecular cancer therapeutics 2016, 15 (6), 1311-1320.

19. Ritchie, M.; Tchistiakova, L.; Scott, N. In Implications of receptor-mediated endocytosis and intracellular trafficking dynamics in the development of antibody drug conjugates, MAbs, Taylor & Francis: 2013; pp 13-21.

20. Erickson, H. K.; Park, P. U.; Widdison, W. C.; Kovtun, Y. V.; Garrett, L. M.; Hoffman, K.; Lutz, R. J.; Goldmacher, V. S.; Blättler, W. A., Antibody-maytansinoid conjugates are activated in targeted cancer cells by lysosomal degradation and linker-dependent intracellular processing. Cancer research 2006, 66 (8), 4426-4433.

21. Erickson, H. K.; Lambert, J. M., ADME of antibody–maytansinoid conjugates. The AAPS journal 2012, 14 (4), 799-805.

22. Perez, H. L.; Cardarelli, P. M.; Deshpande, S.; Gangwar, S.; Schroeder, G. M.; Vite, G. D.; Borzilleri, R. M., Antibody–drug conjugates: current status and future directions. Drug discovery today 2014, 19 (7), 869-881.

23. Jain, N.; Smith, S. W.; Ghone, S.; Tomczuk, B., Current ADC linker chemistry. Pharmaceutical research 2015, 32 (11), 3526-3540.

24. Joubert, M. K.; Hokom, M.; Eakin, C.; Zhou, L.; Deshpande, M.; Baker, M. P.; Goletz, T. J.; Kerwin, B. A.; Chirmule, N.; Narhi, L. O., Highly aggregated antibody therapeutics can enhance the in vitro innate and late-stage T-cell immune responses. Journal of Biological Chemistry 2012, 287 (30), 25266-25279.

25. Kovtun, Y. V.; Audette, C. A.; Mayo, M. F.; Jones, G. E.; Doherty, H.; Maloney, E. K.; Erickson, H. K.; Sun, X.; Wilhelm, S.; Ab, O., Antibody-maytansinoid conjugates designed to bypass multidrug resistance. Cancer research 2010, 70 (6), 2528-2537.

26. Lambert, J. M.; Chari, R. V., Ado-trastuzumab Emtansine (T-DM1): an antibody–drug conjugate (ADC) for HER2-positive breast cancer. ACS Publications: 2014.

27. Senter, P. D.; Sievers, E. L., The discovery and development of brentuximab vedotin for use in relapsed Hodgkin lymphoma and systemic anaplastic large cell lymphoma. Nature biotechnology 2012, 30 (7), 631.

28. Smith, A. L.; Nicolaou, K., The enediyne antibiotics. Journal of medicinal chemistry 1996, 39 (11), 2103-2117.

29. Pettit, G. R.; Kamano, Y.; Herald, C. L.; Tuinman, A. A.; Boettner, F. E.; Kizu, H.; Schmidt, J. M.; Baczynskyj, L.; Tomer, K. B.; Bontems, R. J., The isolation and structure of a remarkable marine animal antineoplastic constituent: dolastatin 10. Journal of the American Chemical Society 1987, 109 (22), 6883-6885.

30. Widdison, W. C.; Wilhelm, S. D.; Cavanagh, E. E.; Whiteman, K. R.; Leece, B. A.; Kovtun, Y.; Goldmacher, V. S.; Xie, H.; Steeves, R. M.; Lutz, R. J., Semisynthetic maytansine analogues for the targeted treatment of cancer. Journal of medicinal chemistry 2006, 49 (14), 4392-4408.

31. Kupchan, S. M.; Sneden, A. T.; Branfman, A. R.; Howie, G. A.; Rebhun, L. I.; McIvor, W. E.; Wang, R. W.; Schnaitman, T. C., Tumor inhibitors. 124. Structural requirements for antileukemic activity among the naturally occurring and semisynthetic maytansinoids. Journal of medicinal chemistry 1978, 21 (1), 31-37.

32. Polakis, P., Antibody drug conjugates for cancer therapy. Pharmacological reviews 2016, 68 (1), 3-19.

33. Barok, M.; Joensuu, H.; Isola, J., Trastuzumab emtansine: mechanisms of action and drug resistance. Breast cancer research 2014, 16 (2), 209.

34. Valliere-Douglass, J. F.; Hengel, S. M.; Pan, L. Y., Approaches to interchain cysteine-linked ADC characterization by mass spectrometry. Molecular pharmaceutics 2014, 12 (6), 1774-1783.

35. Behrens, C. R.; Ha, E. H.; Chinn, L. L.; Bowers, S.; Probst, G.; Fitch-Bruhns, M.; Monteon, J.; Valdiosera, A.; Bermudez, A.; Liao-Chan, S., Antibody–drug conjugates (ADCs) derived from interchain cysteine cross-linking demonstrate improved homogeneity and other pharmacological properties over conventional heterogeneous ADCs. Molecular pharmaceutics 2015, 12 (11), 3986-3998.

36. Sadowsky, J. D.; Pillow, T. H.; Chen, J.; Fan, F.; He, C.; Wang, Y.; Yan, G.; Yao, H.; Xu, Z.; Martin, S., Development of Efficient Chemistry to Generate Site-Specific Disulfide-Linked Protein–and Peptide–Payload Conjugates: Application to THIOMAB Antibody–Drug Conjugates. Bioconjugate chemistry 2017, 28 (8), 2086-2098.

37. Yao, H.; Jiang, F.; Lu, A.; Zhang, G., Methods to design and synthesize antibody-drug conjugates (ADCs). International journal of molecular sciences 2016, 17 (2), 194.

38. Guo, J.; Kumar, S.; Chipley, M.; Marcq, O.; Gupta, D.; Jin, Z.; Tomar, D. S.; Swabowski, C.; Smith, J.; Starkey, J. A., Characterization and higher-order structure assessment of an interchain cysteine-based ADC: impact of drug loading and distribution on the mechanism of aggregation. Bioconjugate chemistry 2016, 27 (3), 604-615.

39. Sievers, E. L.; Senter, P. D., Antibody-drug conjugates in cancer therapy. Annual review of medicine 2013, 64, 15-29.

40. Hamblett, K. J.; Senter, P. D.; Chace, D. F.; Sun, M. M.; Lenox, J.; Cerveny, C. G.; Kissler, K. M.; Bernhardt, S. X.; Kopcha, A. K.; Zabinski, R. F., Effects of drug loading on the antitumor activity of a monoclonal antibody drug conjugate. Clinical cancer research 2004, 10 (20), 7063-7070.

41. Strop, P.; Liu, S.-H.; Dorywalska, M.; Delaria, K.; Dushin, R. G.; Tran, T.-T.; Ho, W.-H.; Farias, S.; Casas, M. G.; Abdiche, Y., Location matters: site of conjugation modulates stability and pharmacokinetics of antibody drug conjugates. Chemistry & biology 2013, 20 (2), 161-167.

42. Wei, C.; Zhang, G.; Clark, T.; Barletta, F.; Tumey, L. N.; Rago, B.; Hansel, S.; Han, X., Where did the linker-payload go? A quantitative investigation on the destination of the released linker-payload from an antibody-drug conjugate with a maleimide linker in plasma. Analytical chemistry 2016, 88 (9), 4979-4986.

43. Nunes, J. P.; Morais, M.; Vassileva, V.; Robinson, E.; Rajkumar, V. S.; Smith, M. E.; Pedley, R. B.; Caddick, S.; Baker, J. R.; Chudasama, V., Functional native disulfide bridging enables delivery of a potent, stable and targeted antibody–drug conjugate (ADC). Chemical Communications 2015, 51 (53), 10624-10627.

44. Baldwin, A. D.; Kiick, K. L., Tunable degradation of maleimide–thiol adducts in reducing environments. Bioconjugate chemistry 2011, 22 (10), 1946-1953.

45. Shen, B.-Q.; Xu, K.; Liu, L.; Raab, H.; Bhakta, S.; Kenrick, M.; Parsons-Reponte, K. L.; Tien, J.; Yu, S.-F.; Mai, E., Conjugation site modulates the in vivo stability and therapeutic activity of antibody-drug conjugates. Nature biotechnology 2012, 30 (2), 184.

46. Ouyang, J., Drug-to-antibody ratio (DAR) and drug load distribution by hydrophobic interaction chromatography and reversed phase high-performance liquid chromatography. In Antibody-Drug Conjugates, Springer: 2013; pp 275-283.

47. Fekete, S.; Veuthey, J.-L.; Beck, A.; Guillarme, D., Hydrophobic interaction chromatography for the characterization of monoclonal antibodies and related products. Journal of pharmaceutical and biomedical analysis 2016, 130, 3-18.

48. Xu, K.; Liu, L.; Dere, R.; Mai, E.; Erickson, R.; Hendricks, A.; Lin, K.; Junutula, J. R.; Kaur, S., Characterization of the drug-to-antibody ratio distribution for antibody–drug conjugates in plasma/serum. Bioanalysis 2013, 5 (9), 1057-1071.

49. Wagner-Rousset, E.; Janin-Bussat, M.-C.; Colas, O.; Excoffier, M.; Ayoub, D.; Haeuw, J.-F.; Rilatt, I.; Perez, M.; Corvaïa, N.; Beck, A. In Antibody-drug conjugate model fast characterization by LC-MS following IdeS proteolytic digestion, MAbs, Taylor & Francis: 2014; pp 173-184.

50. Alley, S. C.; Anderson, K. E., Analytical and bioanalytical technologies for characterizing antibody–drug conjugates. Current opinion in chemical biology 2013, 17 (3), 406-411.

51. Said, N.; Gahoual, R.; Kuhn, L.; Beck, A.; François, Y.-N.; Leize-Wagner, E., Structural characterization of antibody drug conjugate by a combination of intact, middle-up and bottom-up techniques using sheathless capillary electrophoresis–Tandem mass spectrometry as nanoESI infusion platform and separation method. Analytica chimica acta 2016, 918, 50-59.

52. Chen, J.; Yin, S.; Wu, Y.; Ouyang, J., Development of a native nanoelectrospray mass spectrometry method for determination of the drug-to-antibody ratio of antibody–drug conjugates. Analytical chemistry 2013, 85 (3), 1699-1704.

53. Li, Y.; Stella, C.; Zheng, L.; Bechtel, C.; Gruenhagen, J.; Jacobson, F.; Medley, C. D., Investigation of low recovery in the free drug assay for antibody drug conjugates by size exclusion—reversed phase two dimensional-liquid chromatography. Journal of Chromatography B 2016, 1032, 112-118.

54. Pan, L. Y.; Salas-Solano, O.; Valliere-Douglass, J. F., Conformation and dynamics of interchain cysteine-linked antibody-drug conjugates as revealed by hydrogen/deuterium exchange mass spectrometry. Analytical chemistry 2014, 86 (5), 2657-2664.

55. Liu, A.; Kozhich, A.; Passmore, D.; Gu, H.; Wong, R.; Zambito, F.; Rangan, V. S.; Myler, H.; Aubry, A.-F.; Arnold, M. E., Quantitative bioanalysis of antibody-conjugated payload in monkey plasma using a hybrid immuno-capture LC–MS/MS approach: assay development, validation, and a case study. Journal of Chromatography B 2015, 1002, 54-62.

56. Hengel, S. M.; Sanderson, R.; Valliere-Douglass, J.; Nicholas, N.; Leiske, C.; Alley, S. C., Measurement of in vivo drug load distribution of cysteine-linked antibody–drug conjugates using microscale liquid chromatography mass spectrometry. Analytical chemistry 2014, 86 (7), 3420-3425.

57. Torre, L. A.; Siegel, R. L.; Jemal, A., Lung cancer statistics. In Lung cancer and personalized medicine, Springer: 2016; pp 1-19.

58. Siegel, R. L.; Miller, K. D.; Jemal, A., Cancer statistics, 2018. CA: a cancer journal for clinicians 2018, 68 (1), 7-30.

59. Lemjabbar-Alaoui, H.; Hassan, O. U.; Yang, Y.-W.; Buchanan, P., Lung cancer: Biology and treatment options. Biochimica et Biophysica Acta (BBA)-Reviews on Cancer 2015, 1856 (2), 189-210.

60. Schiller, J. H.; Harrington, D.; Belani, C. P.; Langer, C.; Sandler, A.; Krook, J.; Zhu, J.; Johnson, D. H., Comparison of four chemotherapy regimens for advanced non–small-cell lung cancer. New England Journal of Medicine 2002, 346 (2), 92-98.

61. Samson, D. J.; Seidenfeld, J.; Ziegler, K.; Aronson, N., Chemotherapy sensitivity and resistance assays: a systematic review. Journal of clinical oncology 2004, 22 (17), 3618-3630.

62. Moxley, K. M.; McMeekin, D. S., Endometrial carcinoma: a review of chemotherapy, drug resistance, and the search for new agents. The oncologist 2010, 15 (10), 1026-1033.

63. Florea, A.-M.; Büsselberg, D., Cisplatin as an anti-tumor drug: cellular mechanisms of activity, drug resistance and induced side effects. Cancers 2011, 3 (1), 1351-1371.

64. Grilli, R.; Oxman, A. D.; Julian, J. A., Chemotherapy for advanced non-small-cell lung cancer: how much benefit is enough? Journal of clinical oncology 1993, 11 (10), 1866-1872.

65. Chang, A., Chemotherapy, chemoresistance and the changing treatment landscape for NSCLC. Lung cancer 2011, 71 (1), 3-10.

66. Stewart, E. L.; Tan, S. Z.; Liu, G.; Tsao, M.-S., Known and putative mechanisms of resistance to EGFR targeted therapies in NSCLC patients with EGFR mutations—a review. Translational lung cancer research 2015, 4 (1), 67.

67. Gazdar, A. F.; Minna, J. D., Deregulated EGFR signaling during lung cancer progression: mutations, amplicons, and autocrine loops. Cancer Prevention Research 2008, 1 (3), 156-160.

68. Carpenter, G.; Cohen, S., Epidermal growth factor. Annual review of biochemistry 1979, 48 (1), 193-216.

69. Mukohara, T.; Kudoh, S.; Yamauchi, S.; Kimura, T.; Yoshimura, N.; Kanazawa, H.; Hirata, K.; Wanibuchi, H.; Fukushima, S.; Inoue, K., Expression of epidermal growth factor receptor (EGFR) and downstream-activated peptides in surgically excised non-small-cell lung cancer (NSCLC). Lung cancer 2003, 41 (2), 123-130.

70. Talavera, A.; Friemann, R.; Gómez-Puerta, S.; Martinez-Fleites, C.; Garrido, G.; Rabasa, A.; López-Requena, A.; Pupo, A.; Johansen, R. F.; Sánchez, O., Nimotuzumab, an antitumor antibody that targets the epidermal growth factor receptor, blocks ligand binding while permitting the active receptor conformation. Cancer research 2009, 69 (14), 5851-5859.

71. Fojo, T.; Grady, C., How much is life worth: cetuximab, non–small cell lung cancer, and the $440 billion question. Journal of the National Cancer Institute 2009, 101 (15), 1044-1048.

72. Patel, D.; Lahiji, A.; Patel, S.; Franklin, M.; Jimenez, X.; Hicklin, D. J.; Kang, X., Monoclonal antibody cetuximab binds to and down-regulates constitutively activated epidermal growth factor receptor vIII on the cell surface. Anticancer research 2007, 27 (5A), 3355-3366.

73. Xue, L.-y.; Chiu, S.-m.; Oleinick, N. L., Staurosporine-induced death of MCF-7 human breast cancer cells: a distinction between caspase-3-dependent steps of apoptosis and the critical lethal lesions. Experimental cell research 2003, 283 (2), 135-145.

74. Gescher, A., Staurosporine analogues—pharmacological toys or useful antitumour agents? Critical reviews in oncology/hematology 2000, 34 (2), 127-135.

75. Bertrand, R.; Solary, E.; O'Connor, P.; Kohn, K. W.; Pommier, Y., Induction of a common pathway of apoptosis by staurosporine. Experimental cell research 1994, 211 (2), 314-321.

76. Lawrie, A. M.; Noble, M.; Tunnah, P.; Brown, N. R.; Johnson, L. N.; Endicott, J. A., Protein kinase inhibition by staurosporine revealed in details of the molecular interaction with CDK2. Nature structural biology 1997, 4 (10), 796-801.

77. Toledo, L. M.; Lydon, N. B., Structures of staurosporine bound to CDK2 and cAPK–new tools for structure-based design of protein kinase inhibitors. Structure 1997, 5 (12), 1551-1556.

78. Qiao, L.; Koutsos, M.; Tsai, L.-L.; Kozoni, V.; Guzman, J.; Shiff, S. J.; Rigas, B., Staurosporine inhibits the proliferation, alters the cell cycle distribution and induces apoptosis in HT-29 human colon adenocarcinoma cells. Cancer letters 1996, 107 (1), 83-89.

79. Courage, C.; Snowden, R.; Gescher, A., Differential effects of staurosporine analogues on cell cycle, growth and viability in A549 cells. British journal of cancer 1996, 74 (8), 1199.

80. Wang, Y.; Yang, H.; Liu, H.; Huang, J.; Song, X., Effect of staurosporine on the mobility and invasiveness of lung adenocarcinoma A549 cells: an in vitro study. BMC cancer 2009, 9 (1), 174.

81. Zhang, X. D.; Gillespie, S. K.; Hersey, P., Staurosporine induces apoptosis of melanoma by both caspase-dependent and-independent apoptotic pathways. Molecular cancer therapeutics 2004, 3 (2), 187-197.

82. Belmokhtar, C. A.; Hillion, J.; Segal-Bendirdjian, E., Staurosporine induces apoptosis through both caspase-dependent and caspase-independent mechanisms. Oncogene 2001, 20 (26), 3354.

VITA

Ke Li was born in Pingdingshan, Hean Province, China. In 2007, he was admitted to the Department of Chemistry, Zhengzhou University, Henan province, China. After he received his BS degree in 2011, he started to work in the pharmaceutical industry for 3.5 years. In 2015, he joined in Missouri University of Science and Technology to continue his study in Drs. Yinfa Ma and Honglan Shi's group. He received his Ph.D. degree in Chemistry in December 2019 from Missouri University of Science and Technology.